

# Functional Fluorescent Dyes and their Polymer Conjugates

DISSERTATION

zur Erlangung des akademischen Grades des  
Doktors der Naturwissenschaften (Dr. rer. nat.)

eingereicht im Fachbereich Biologie, Chemie, Pharmazie  
am Institut für Chemie und Biochemie  
der Freien Universität Berlin

vorgelegt von  
Virginia Wycisk  
aus Berlin

November 2016

The following PhD Thesis was compiled in the group of Prof. Dr. Rainer Haag in the period from October 2012 until November 2016 at the Institute of Chemistry and Biochemistry of the Freie Universität Berlin.

1st Reviewer: Prof. Dr. Rainer Haag

2nd Reviewer: PD Dr. Kai Licha

Day of Defense: December 16th, 2016

I hereby declare that this PhD thesis is the result of my own research and that all utilized sources and references are acknowledged properly by referring to the original work.

## **Acknowledgements**

First of all, I would like to express my gratitude to Prof. Dr. Rainer Haag for giving me the opportunity to be part of his group and for being my scientific mentor. His financial and scientific support in the past years was very much appreciated. I am infinitely grateful to PD Dr. Kai Licha for his scientific and personal support and for being an excellent supervisor for me through all the years.

Furthermore, I sincerely thank Nicole Wegner, Sylvia Kern, and Ingo Steinke for introducing me to their laboratory and for teaching me all the technical skills. Thank you for your constant help, support, and interest in my work. Further thanks go to my other lab colleagues, Nadine Rades, Cathleen Schlesener and Benjamin Ziem, for the nice atmosphere and useful scientific as well as private discussions.

In addition, I would like to thank all former and present members of the Haag group, particularly Dr. Katharina Achazi who has been a great help in conducting the biological experiments as well as a strong support and good friend since the beginning of my PhD. The multivalency subgroup is acknowledged for their help and support through all the years. Dr. Pamela Winchester I want to thank for proofreading my thesis and manuscripts. Sincere thanks go to Jutta Hass and Dr. Wiebke Fischer for helping me with financial support and complicated paper work as well as other issues.

Dr. Jens Dervedde and Christian Kühne from the Charité Berlin are thanked for teaching me protein purification and analysis and for their kind help and support. I am further grateful to Dr. Ole Hirsch (PTB) for his kind help with fluorescence measurements and further result discussions.

The analytical department of the Institute of Chemistry and Biochemistry is acknowledged for numerous NMR and MS measurements. I am grateful for the financial support received from the Dahlem Research School and the Helmholtz Association for funding this work through the Helmholtz-Portfolio Topic “Multimodal Imaging”.

Many thanks go to the “Lunch Group” for the fun and good company we had inside and outside of university. I especially want to thank Era Kapourani and Nadine Rades for becoming close friends of mine and for their continuous support in personal life.

Special thanks go to my family for their personal and financial support during my whole education. I especially want to thank my parents for their continuous love, care and understanding throughout all these years.

Finally, I am eternally grateful to Leonhard Urner for his love and personal support. Your encouragement and motivation helped me to go through the most difficult times during my PhD. Thank you for the great time we had the past two years and I am looking forward to the ones coming.

# Table of Contents

<b>1 INTRODUCTION.....</b>	<b>1</b>
1.1 Fluorescence and Principles .....	1
1.2 Fluorescence and its Application in Biomedical Imaging.....	2
1.2.1 <i>Optical Imaging</i> .....	3
1.2.2 <i>Imaging Probes</i> .....	3
1.3 Cyanine Dyes.....	8
1.3.1 <i>Structural Characteristics</i> .....	8
1.3.2 <i>Synthetic Approaches to Indocarbocyanines</i> .....	11
1.3.3 <i>Functionalization of Indocarbocyanines</i> .....	12
1.3.4 <i>Optical Properties and Aggregation Behavior</i> .....	17
1.3.5 <i>Responsive Cyanine Dyes</i> .....	25
1.3.6 <i>Activatable Probes based on Cyanines</i> .....	28
<b>2 MOTIVATION AND OBJECTIVES.....</b>	<b>32</b>
<b>3 PUBLICATIONS AND MANUSCRIPTS .....</b>	<b>34</b>
3.1 Glycerol-Based Contrast Agents: A Novel Series of Dendronized Pentamethine Dyes .....	34
3.2 Responsive Contrast Agents: Synthesis and Characterization of a Tunable Series of pH-Sensitive Near-Infrared pentamethines .....	49
3.3 Heterobifunctional dyes: Highly Fluorescent Linkers Based on Cyanine Dyes ...	72
<b>4 SUMMARY AND CONCLUSION.....</b>	<b>101</b>
<b>5 OUTLOOK .....</b>	<b>104</b>
<b>6 KURZZUSAMMENFASSUNG.....</b>	<b>106</b>
<b>7 REFERENCES .....</b>	<b>109</b>
<b>8 APPENDIX .....</b>	<b>116</b>
8.1 List of Abbreviations .....	116
8.2 List of Publications.....	117
8.3 Manuscripts in Preparation.....	117
8.4 Curriculum Vitae .....	118

# 1 INTRODUCTION

## 1.1 Fluorescence and Principles

Fluorescence is a phenomenon, which can often be observed in nature, such as some sea organisms and more commonly in Green Fluorescent Protein (GFP) which exhibits bright green fluorescence.<sup>[1]</sup> Generally, a fluorescent molecule, also known as fluorophore, emits light from a previously absorbed photon. Upon interaction with light, an electron is promoted from the ground state ( $S_0$ ) to an excited state of high energy ( $S_1$  or  $S_2$ ) in a rapid transition. Emission of light occurs when the electron relaxes to its ground state, which occurs within nanoseconds. In many cases, the energy of emitted light is lower than the absorbed radiation, which results in emission at longer wavelengths. This effect is called Stokes shift and is determined as the difference between absorption and fluorescence maximum which is strongly influenced by the fluorophore's structure.<sup>[2]</sup>

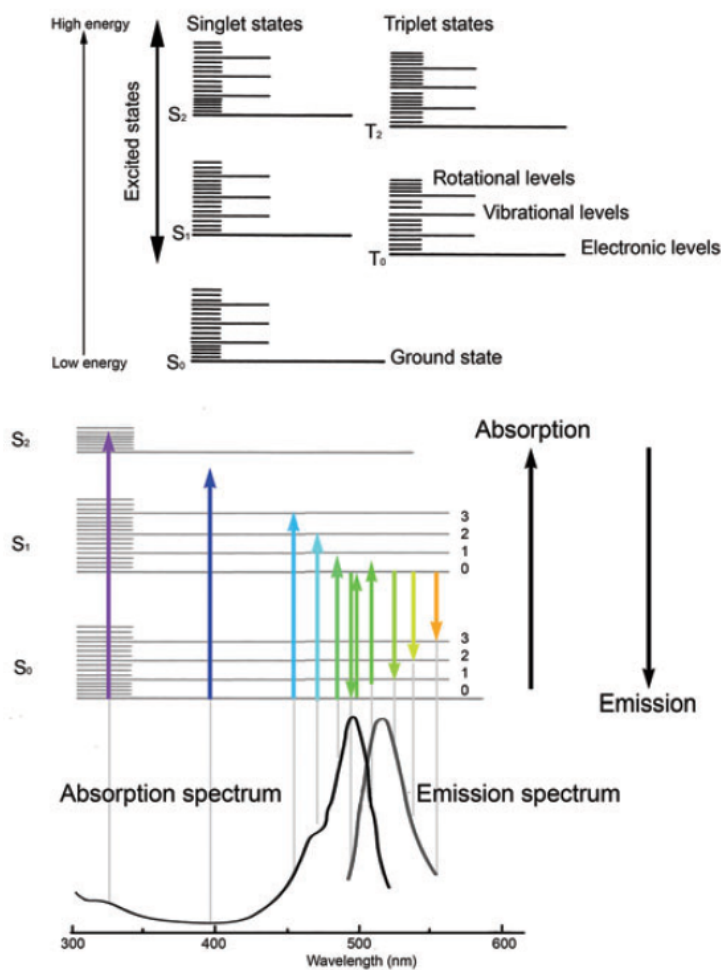


**Figure 1.** Jablonski diagram illustrating the energy levels and the possible transitions during absorption and emission. Adapted with permission from Lichtman et al.<sup>[3]</sup>

The loss of energy is caused by vibrational relaxation of electrons from high vibration levels to the lowest vibration level of the excited state (non-radiative transition). Each vibrational level is associated with several rotational levels resulting in many possible transitions from the ground states. Generally, absorption spectra reveal broad peaks due to difficulties in resolving individual transitions as sharp bands except for compounds with restricted rotational levels.<sup>[3]</sup> A useful tool for the understanding of electronic transitions is the Jablonski diagram shown in Figure 1 which was designed by Alexander Jablonski in the 1930s.<sup>[2]</sup> Another pathway of relaxation from the excited to the ground state is internal conversion where the electron converts from the lowest vibrational level of the high-energy state to the highest vibrational level of a lower energy state. No energy is lost during the conversion because the energy of both levels is similar. Extra energy is emitted, however, by interaction with solvents.<sup>[3]</sup> Strong fluorophores usually emit photons in the final transition back to the ground state. A measurement of the efficiency of fluorescence is determined as fluorescence quantum yield ( $\phi_f$ ), which is defined as the ratio of absorbed photons to emitted photons (Equation 1). The number of absorbed photons is determined as molar absorption coefficient  $\epsilon$  of a fluorophore. The higher the coefficient the better is the absorbance of the fluorophore at a specific wavelength. The number of emitted photons is determined as the total light emitted over the entire fluorescence spectral range.

$$\phi_f = \frac{\text{Number of absorbed photons}}{\text{Number of emitted photons}} \quad (\text{Eq. 1.})$$

The product of the molar absorption coefficient and fluorescent quantum yield is defined as brightness and used as measure for the fluorescence output of the fluorophore at a specific wavelength. The time the fluorophore remains in the excited state is defined as fluorescence lifetime. Typically, fluorophores exhibit short lifetimes of several nanoseconds before they finally drop to the ground state.<sup>[3]</sup> Molecules in the excited state can also excite nearby fluorophores, which then emits a photon. This phenomenon is known as fluorescence resonance energy transfer (FRET) and strongly depends on the distance of the donor and acceptor fluorophore. The process occurs when both fluorophores arrange in a close proximity and the acceptor's emission spectrum overlaps with the donor's absorption spectrum.<sup>[4]</sup>

## 1.2 Fluorescence and its Application in Biomedical Imaging

During the past century, the use of fluorescent light has been studied enormously as an analytical technique, but its application as an imaging method was established slowly. The



development of the first fluorescence spectrometer and microscope raised the interest in the technique for the investigation of cellular compartments.<sup>[5]</sup> Nowadays, modern medicine and science and particularly clinical diagnosis rely on fluorescence spectroscopy, imaging, and fluorescent probes.<sup>[6]</sup> Fluorophores are broadly applied in enzyme-linked immunosorbent assay (ELISA) and provide a safer alternative to the previously used immunoassays based on the measurement of radioactivity.<sup>[7]</sup> The development of new laser technology and sophisticated optical devices facilitated the use of fluorescence imaging techniques and revealed a detailed insight into the morphology of living cells. Moreover, the development of stimulated emission depletion (STED) microscope by Stefan Hell allowed for high resolution fluorescence microscopy by bypassing the diffraction limit of light microscopy and was awarded with the Nobel Prize in 2014.<sup>[8]</sup>

### **1.2.1 Optical Imaging**

The use of fluorescence in optical imaging techniques reveals information on tissue anatomy, physiology, as well as metabolic and molecular function. Particularly, in clinical research, these imaging methods have given rise to much interest due to their inexpensiveness, ease to operate, and rather simple instrumentation. However, the most important advantage is application of non-ionizing and harmless radiation as well as fluorescent labels in low concentrations. Furthermore, optical imaging has to fulfill the following criteria: (a) allow early detection and (b) precisely locate the diseased tissue. Nowadays, instruments are broadly applied in animal research and clinical diagnostics including animal scanners and devices for endoscopy, surgery, and joint inflammation detection.<sup>[6,9-10]</sup> Generally, fluorescence devices are applied for fluorescence reflectance imaging, bioluminescence imaging, and for measurements of fluorescence intensity and lifetime.<sup>[6]</sup> For all these measurements, it is crucial to achieve a high signal intensity of the diseased over normal tissue area (signal-to-noise ratio, SNR). Optimal SNR are obtained by notable signal accumulation in the target area.

### **1.2.2 Imaging Probes**

Within the scope of this work, imaging probes are considered those, which are exogenously applied or injected, whereas the broad field of genetically encoded fluorescent proteins, as described above, are not further addressed. Generally, injectable imaging probes must meet several demands including good water solubility and low absorption out of the range of autofluorescence of cells and tissue.<sup>[11]</sup> Moreover, high fluorescence quantum yield, long fluorescence lifetime, and good photostability are the major requirements for good imaging

probes.<sup>[12]</sup> Nowadays, imaging probes contain a variety of different fluorophores such as fluorescent nanoparticles, quantum dots, and nanocrystalline materials, whereas organic dyes are more broadly applied in optical imaging techniques due to versatile design strategies. Widely established classes of organic fluorophores are xanthene and polymethine dyes and less frequently used are boron-dipyrromethenes (BODIPYs), squaraine dyes, and, in some cases, (benzo)phenoxazines and (benzo)phenoxazones (see Figure 2).<sup>[6]</sup>

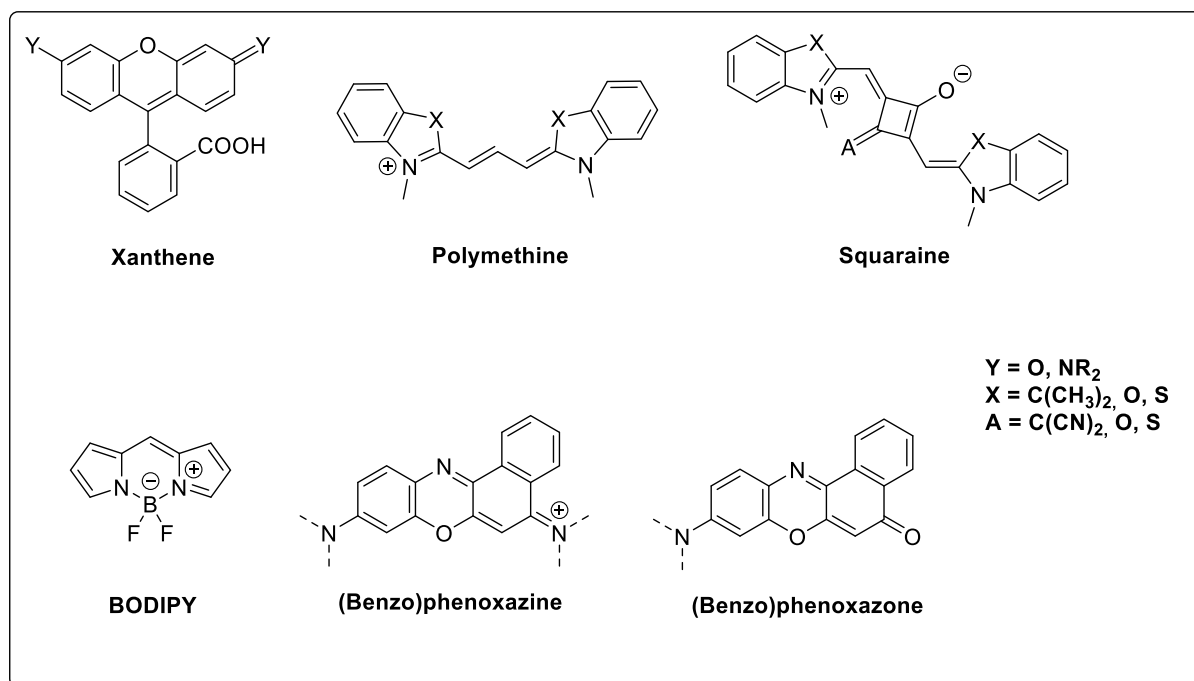


**Figure 2.** Different classes of organic fluorophores applied in optical imaging.

Among them are cyanine dyes belonging to the huge class of polymethines, which evoked major interest in the past century. Indocyanine green (ICG) illustrated in Figure 3 is the most prominent example, not only because of its near-infrared (NIR) emission allowing for imaging in the optical window of tissue (650 – 1450 nm)<sup>[13]</sup> but also because it is the only clinically approved cyanine dye.<sup>[14]</sup> ICG was originally designed as a blood-pooling agent and is nowadays applied as diagnostic imaging probe including fluorescence angiography in ophthalmology,<sup>[15]</sup> imaging of lymphoid disorders,<sup>[16]</sup> or fluorescence-guided surgery.<sup>[9]</sup>

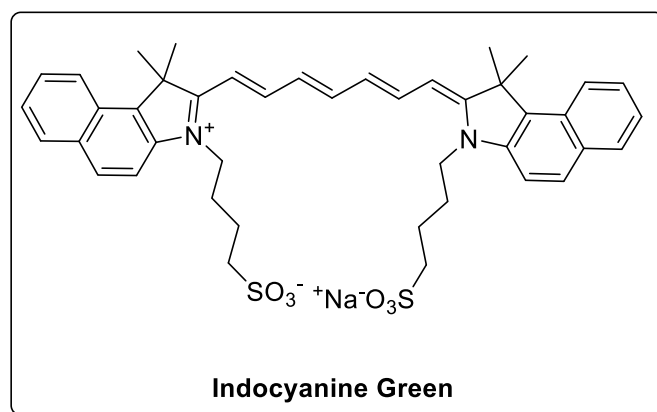


**Figure 3.** Chemical structure of Indocyanine green.

The reduced bioavailability as well as its suffering from poor photostability, pronounced aggregation tendency and low fluorescence quantum yield make it unattractive for modern optical imaging.<sup>[11]</sup> Furthermore, in its use as a non-specific contrast agent, ICG binds to many serum proteins, but its high plasma protein binding has proven disadvantageous. The contrast agent lacks any reactive functional groups for further bioconjugation and therefore does not target-specifically accumulate *in vivo*.<sup>[12]</sup> The attachment of a reactive group inside the fluorophore for subsequent conjugation to a targeting or carrier unit is a commonly used method to generate specific optical imaging probes. Figure 4 illustrates the covalent attachment strategies of a fluorophore R with a targeting moiety (circle). The fluorescent label generally provides (a) maleimides, (b) N-hydroxysuccinimide (NHS) ester, (c) isothiocyanates or (d) amines for reactions with biomolecules under physiological condition. In case of biomolecule labeling, amino acid residues, e.g. thiols (cysteine), amines (lysine), or alcohols (threonine, serine or glycans) provide good reaction partners for the above-mentioned groups. Moreover, by modification of the targeting system, the labels can also be attached via cycloadditions (e) - (g) in a biorthogonal way.<sup>[6]</sup>

Accumulation of the probe at the target site, e.g., diseased tissue leads to enhanced signal intensity. However, the use of these so-called “always on” probes is detrimental, because their emission is not influenced by interaction with targeted tissue or cells. Therefore, they generate a low signal-over-noise level. Of great interest for the application of fluorescence is the ability to make use of molecular interactions that influence the fluorescence properties, which are usually highly dependent on the local chemical environment. In that respect, an emerging approach has been the design of activatable probes consisting of a non-emissive fluorophore that becomes highly emissive upon chemical modification or release from a carrier system at the target side.

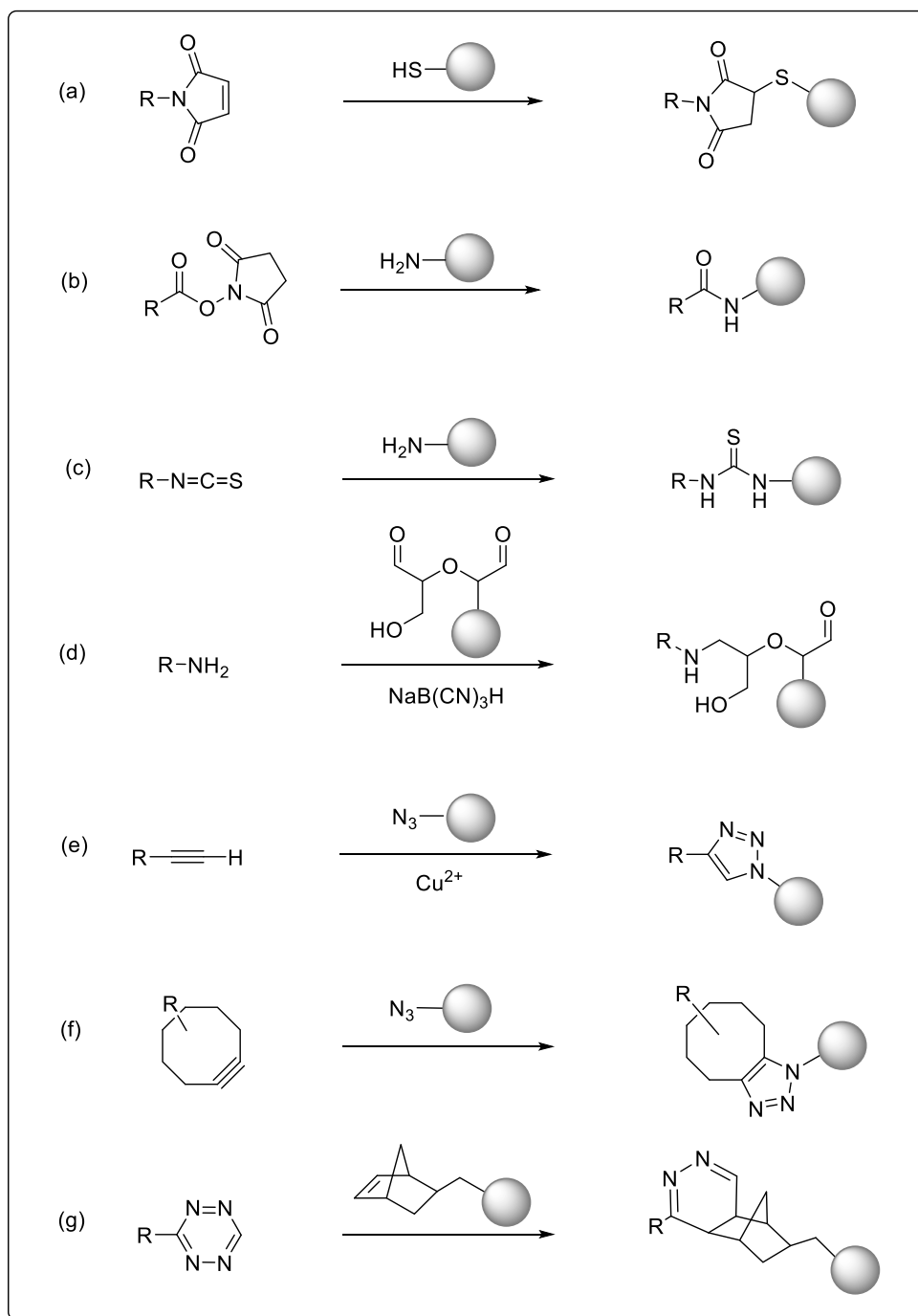


**Figure 4.** Schematic presentation of possible labeling strategies: (a) Michael addition, (b) amide formation, (c) isothiocyanate, amine reaction, (d) reductive amination, (e) copper-catalyzed click reaction, (f) strain-promoted click reaction, (g) tetrazine, alkenyl cycloaddition.<sup>[6]</sup>

The emission is triggered by an environmental change which can be achieved by enzymatic digestion, acidification, oxidation, thiol recognition, or ion complexation (see Figure 5).<sup>[11,14]</sup> Basic concepts consist of sensor probes with a built-in sensor function used as reversible or irreversible trigger. A specific chemical structure is incorporated in the fluorophore with a direct effect on the  $\pi$ -system leading to a diminished emission. In response to the chemical

environment, the fluorophore is chemically converted into a strong emitting probe by a change in or restorage of the  $\pi$ -system.<sup>[6,17]</sup> In the other approach, the fluorophore is embedded in a cleavable matrix like a polymer thereby revealing low emission signals due to intermolecular quenching of fluorescence. Usually, chemical modifications of the fluorophore are not required because the dyes form non-emissive aggregates. Upon cleavage or decomposition of the carrier or matrix, e.g. by tumor-specific enzymes, the initially quenched fluorescence is restored resulting in pronounced signals at the target site. In summary, activatable probes enhance the target signal while they decrease the background signal, which leads to high signal-to-noise ratios. The principles described above have all been applied to organic chromophores, with the vast majority of approaches established for the class of cyanine dyes. Accordingly, the following chapter provides an insight particularly on the versatility of cyanine dyes due to many ways to modify this type of chromophore and adapt its chemistry to the demands in the field of optical imaging.

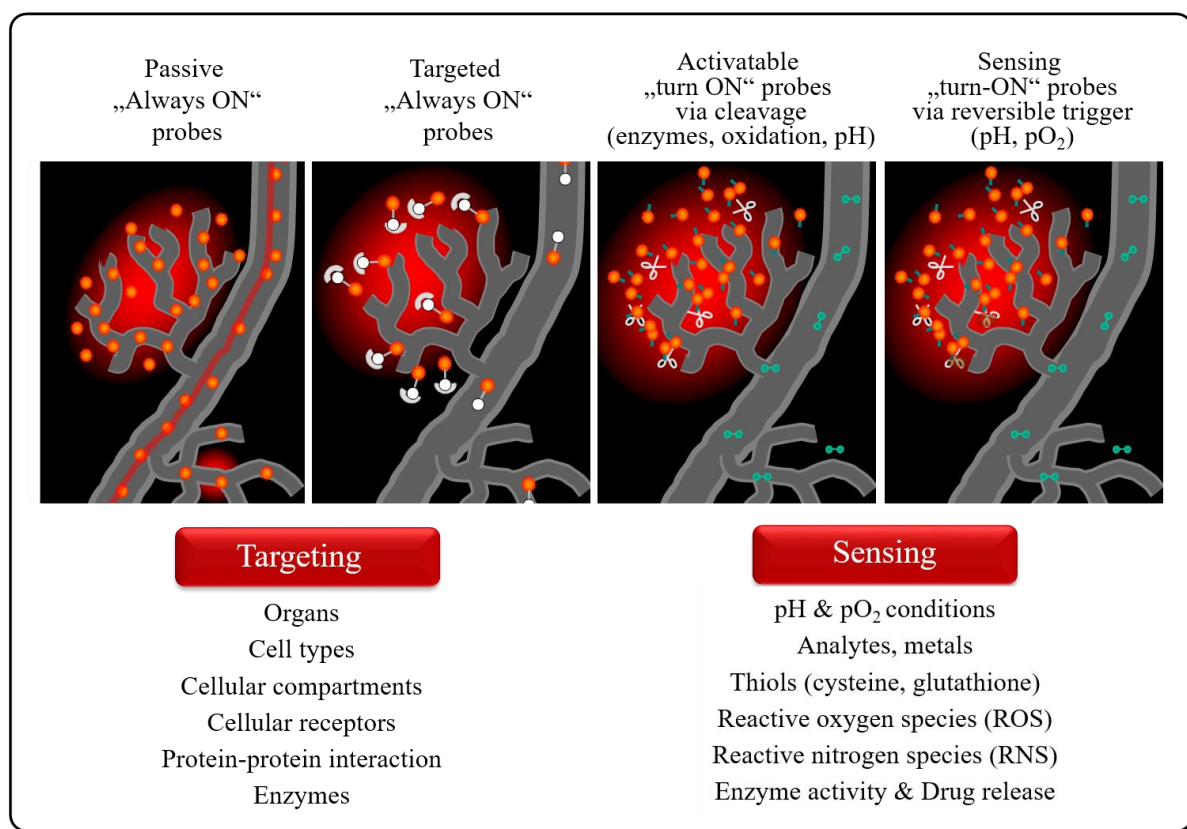


**Figure 5.** Modes of action in vivo adapted with permission from Licha et al.<sup>[11]</sup>

### 1.3 Cyanine Dyes

The name cyanine dye was derived from the Ancient Greek word “κύανος” (kyanos)<sup>[18]</sup> which means dark blue referring to color of very first cyanine, which was discovered in 1856 by G. Williams.<sup>[19]</sup> Originally, cyanine dyes were used as textile dyes, but their application was negligible. Due to their ability to impart light sensitivity, they were soon applied in silver halide photography.<sup>[20]</sup> Nowadays, cyanines are used in semiconducting materials, laser materials, optical recording media, and more recently they were broadly applied in biomedical imaging due to their outstanding fine tuning possibilities.<sup>[21]</sup>

#### 1.3.1 Structural Characteristics

Cyanine dyes belong to the huge group of polymethine dyes, which are characterized by a donor-acceptor pair containing two identical heteroatoms connected by a polymethine chain.<sup>[21]</sup> These dyes usually contain oxygen or nitrogen atoms and are classified as oxonole or cyanine dyes, respectively (see Figure 6). Fluorophores with different heteroatoms are generally known as mero(poly)methines and exhibit nonpolar and zwitterionic resonance structures.<sup>[22]</sup>

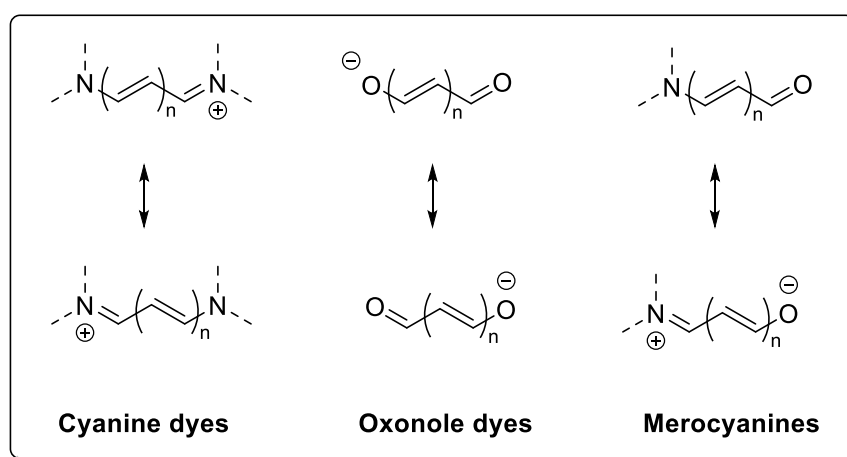


**Figure 6.** Chemical structures of cyanines, oxonoles, and merocyanines (meropolymethines) and their resonance structures.<sup>[22]</sup>

Merocyanines are characterized by terminal nitrogen and oxygen atoms and are sensitive to solvent polarities due to polar and nonpolar structures.<sup>[23]</sup> However, cyanine dyes are only slightly influenced by solvent changes because of the delocalization of the  $\pi$ -system, which is conjugated by two terminal nitrogen atoms acting as electron donor and acceptor. One of the nitrogen centers is quaternary and positively charged and connected to the tertiary nitrogen via a polymethine chain. The polymethine chain consists of an odd number of methine groups and

they are termed according to the number of conjugated carbon atoms as mono-, tri-, penta-, or heptamethines for  $n = 0, 1, 2, 3$ , respectively. Moreover, the dyes can be classified by the substitution of nitrogen atoms, which results in open chain cyanines (streptocyanines) or closed chain cyanines exhibiting two equal or different heterocyclic end groups. Hemicyanines contain one terminal heterocyclic structure while the other nitrogen atoms do not carry any cyclic group, which is shown in Figure 7.<sup>[22]</sup>

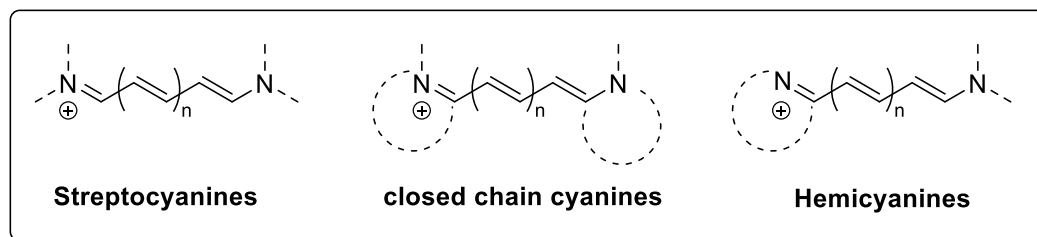


**Figure 7.** Chemical structures of cyanine dyes with different N-substitutions.<sup>[22]</sup>

A variety of heterocyclic groups is illustrated in Figure 8 including quinoline which was the base of the first cyanine dye more than 100 years ago.<sup>[19]</sup> Nowadays, commonly used heterocycles in cyanine dyes for optical imaging are the following: 3*H*-indole, 3*H*-benzindole, benzoxazole, benzothiazole, or benz(*cd*)indoles.<sup>[6,24-25]</sup> Symmetric dyes are characterized by the same terminal groups, while asymmetric dyes contain two differing moieties. Whereas many cyanine dyes have been synthesized in the past years, not every possible combination of the heterocyclic structures displayed in Figure 8 has been achieved. Symmetric dyes were intensively studied by X-ray crystallography and NMR spectroscopy and revealed a planar structure and, moreover, a uniform carbon-carbon bond length with a mean distance of 1.46 Å for thiazolium dyes.<sup>[20,26]</sup>

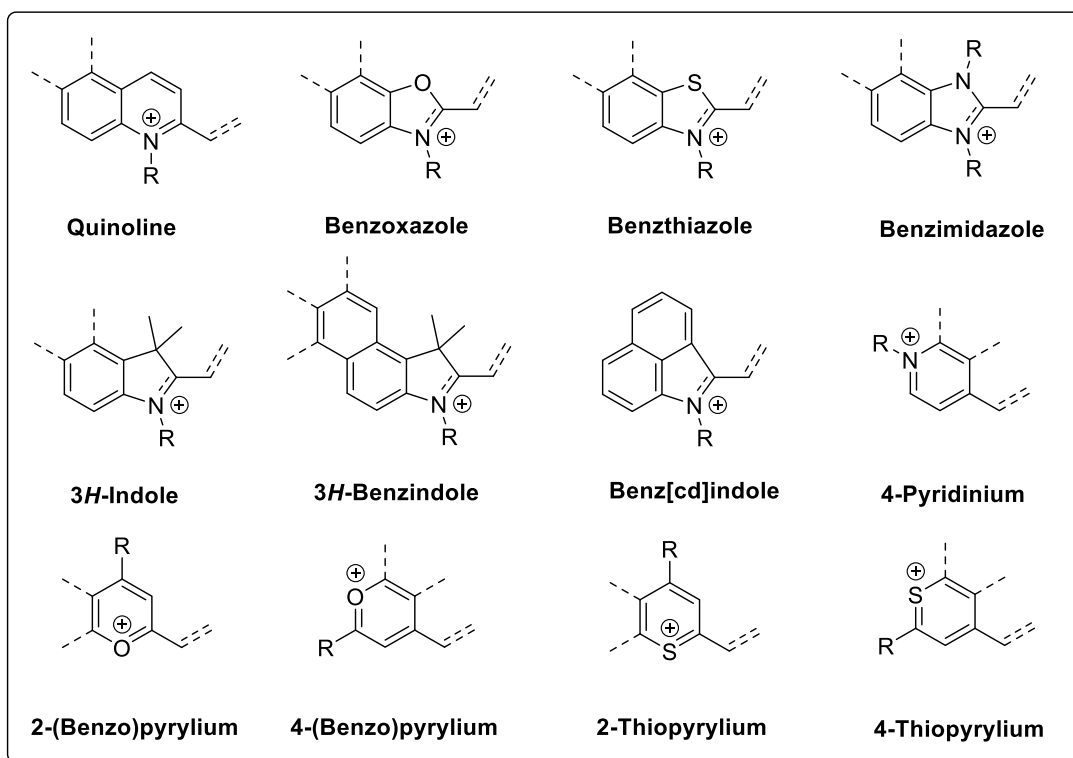


**Figure 8.** Heterocyclic end groups of cyanine dyes<sup>[6]</sup>

Indocarbocyanines can be synthesized as symmetric or asymmetric derivatives and extensions of the conjugated chain are distinguished as the following: Indocarbocyanine (ICC), Indodicarbocyanine (IDCC) or Indotricarbocyanine (ITCC) shown in Figure 9. The stability of cyanine dyes decreases with methine chain length and particularly heptamethine dyes are less stable.<sup>[27]</sup> However, the stability of heptamethine dyes is increased when incorporating a cyclic moiety into the conjugated system, which introduces more rigidity to the system.<sup>[28-30]</sup> Furthermore, indocarbocyanine dyes enable many possibilities for substitutions which will be discussed in the following chapters.

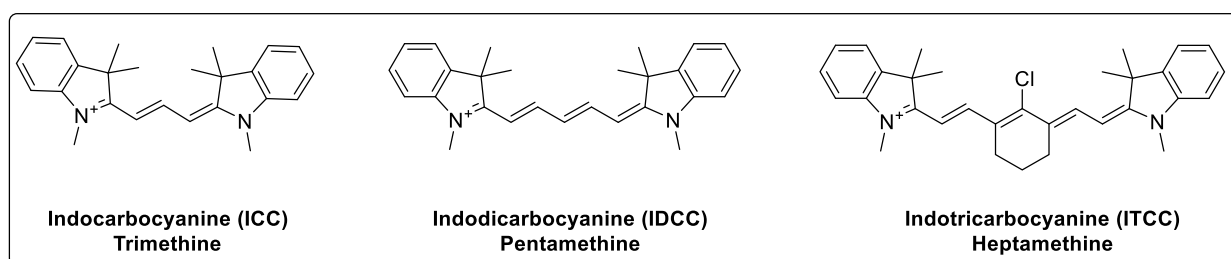


**Figure 9.** Structure of symmetric indocarbocyanines including a heptamethine dye with an incorporated cyclohexyl ring.



### 1.3.2 Synthetic Approaches to Indocarbocyanines

Indocarbocyanines are classically synthesized by condensation under basic conditions using two equivalents of a nucleophilic quaternary salt and an electrophilic reagent. The quaternary salt is usually an active methylene base, e.g., commercially available 2,3,3-trimethylindolenine, also known as Fisher's Base (see Figure 10).

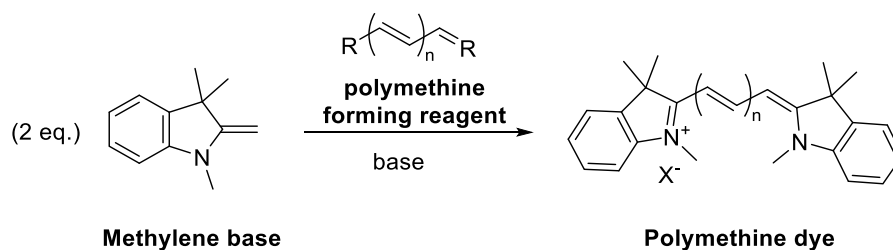


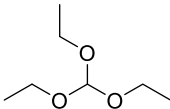
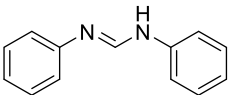
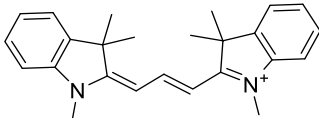
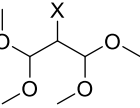
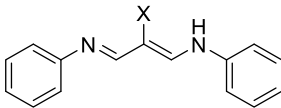
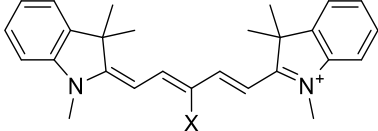
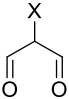
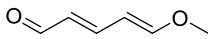
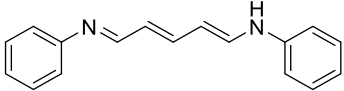
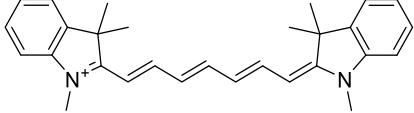
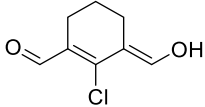
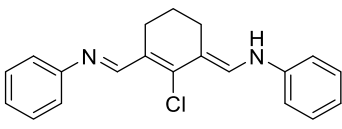
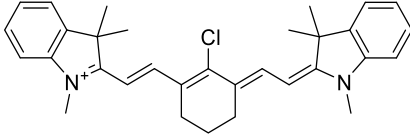
**Figure 10.** General synthesis of cyanine dyes.

Generally, polymethine forming reagents are polyenes with electrophilic leaving groups. A list of polymethine forming reagents for the synthesis of tri- ( $n = 1$ ), penta- ( $n = 2$ ) or heptamethines ( $n = 3$ ) is shown in

Table 1. Symmetric cyanine dyes are yielded after heating in the presence of base, which can be pyridine, sodium acetate, or others.<sup>[20,31]</sup> Historically, trimethines were synthesized from ortho formate, however, in recent papers they are derived from iodoform or N, N'-diphenylformamide, the latter being a more stable and workable analog of an orthoester.<sup>[23,32]</sup> By using malondialdehyde and glutaconic aldehyde derivatives, similarly by protecting them in the format of dianilides, the polymethine system can be increased to yield penta- and heptamethine dyes.<sup>[33-34]</sup> Those reagents can be also used for the synthesis of asymmetric cyanines via the formation of electrophilic intermediates.<sup>[35]</sup> Waggoner et al. presented sufficient synthetic strategies to yield symmetric and asymmetric cyanine dyes from Cy3 to Cy7 range. For the first time, they developed water-soluble cyanine dyes with reactive groups for subsequent labeling of proteins or nucleic acids.<sup>[23, 36-38]</sup> Moreover, they also prepared benzindocyanines with shifted absorption maxima due to the additional benzene substitution of the indolenine.<sup>[39]</sup> As mentioned in the previous chapter, heptamethine dyes are usually prepared with a rigid cyclohexenyl ring in the polymethine chain in order to increase stability. The synthesis was carried out by condensing a Vilsmeier-Haack reagent (glutaconic aldehyde cyclohexene-bridged) with quaternized indolenines to yield chloro-substituted heptamethines,

thereby providing a reactive *meso*-position in the polymethine chain for further derivatization.<sup>[30,40]</sup> Furthermore, Patonay et al. optimized synthetic methods to achieve symmetric and asymmetric heptamethine dyes in high yields (72-95%) by using butanol/benzene mixtures without the requirement of sodium acetate as catalyst.<sup>[41]</sup>

**Table 1.** General components for the synthesis of polymethine dyes

n =	Polymethine forming moiety	Polymethine dye	
1	 <p><b>ortho formate</b></p>	 <p><b>N',N diphenylformamide</b></p>	 <p><b>Trimethine</b></p>
2	 <p><b>Malonaldehyde bis(dimethyl acetal)</b></p>	 <p><b>Anilino acroleine anil</b></p>	 <p><b>Pentamethine</b></p>
	 <p><b>Malondialdehyde</b></p>		
3	 <p><b>Glutaconic aldehyde acetal</b></p>	 <p><b>Glutaconic aldehyde dianilide</b></p>	 <p><b>Heptamethine</b></p>
	 <p><b>Glutaconic aldehyde acetal (cyclohexene-bridged)</b></p>	 <p><b>Glutaconic aldehyde dianilide (cyclohexene-bridged)</b></p>	 <p><b>Heptamethine (cyclohexene-bridged)</b></p>

X = H, Br, Cl, alkyl

### 1.3.3 Functionalization of Indocarbocyanines

While synthetic approaches enable a variation of polymethine chain length, structural diversity of cyanine dyes is mainly achieved by alterations of the heterocycle. The heterocyclic system enables two positions for fine tuning dye properties: the aromatic system and nitrogen substituents. Moreover, the central carbon atom in the polymethine chain can undergo several

modifications. Figure 11 illustrates the three main positions including (a) *meso*-position, (b) the aromatic system, and (c) nitrogen substituents.

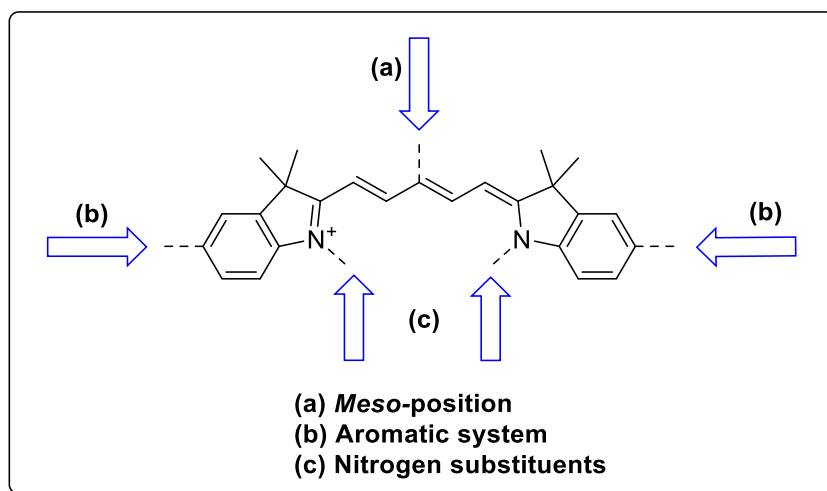


**Figure 11.** Modifications of cyanine dyes at three positions.

Generally, each of these positions must be transferred into a reactive moiety before dye synthesis to prevent the chromophore from degradation due to harsh reaction conditions. For example, cyanine dyes are unstable under aqueous basic conditions<sup>[6]</sup> as nucleophilic addition reactions occur under extreme pH conditions.<sup>[42]</sup>

General synthetic routes to cyanine dyes limit the selection of reactive groups, however, halogen atoms, sulfonic and carboxylic acids are rather inert under these conditions. Therefore they are excellent groups for fine tuning the cyanine dyes. The following subchapters highlight the post-synthetic modification of the three positions discussed here and show the variety of heterocyclic moieties that can be applied for reactive cyanine labels.

#### (a) *Meso*-position

*Meso*-substituted dyes usually contain alkyl groups or halogen atoms. Reactions on *meso*-substituted dyes are generally accomplished by nucleophilic substitution (S<sub>N</sub>) or palladium-catalyzed cross coupling thereby replacing the *meso*-halogen. Furthermore, trimethines can undergo addition reactions employing an already established methyl group used for a condensation with an aldehyde to yield a *meso*-substituted cyanine dye (Figure 12).<sup>[43]</sup>

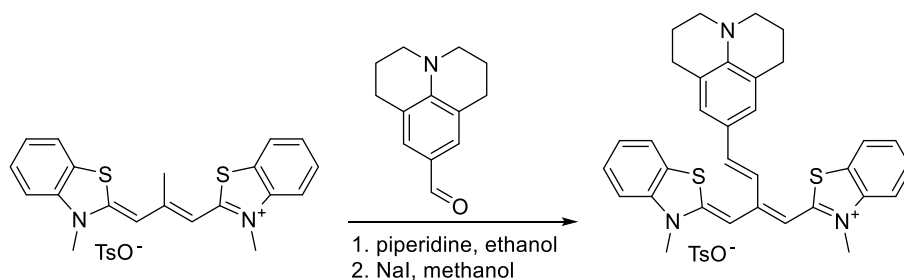


**Figure 12.** Trimethine dyes substituted at the *meso*-position.

Pentamethines can be readily synthesized with *meso*-halogen atoms, which can be further modified by applying palladium-catalyzed cross-coupling reactions. In 1995, Jones et al. showed reactions to *meso*-substituted indocyanines via Stille, Heck, and Sonogashira coupling, which allows one to introduce different types of aromatic moieties (see Figure 13).<sup>[44]</sup> Bromo-substituted pentamethines yielded dyes with C-C bonds at the *meso*-position in moderate yields.

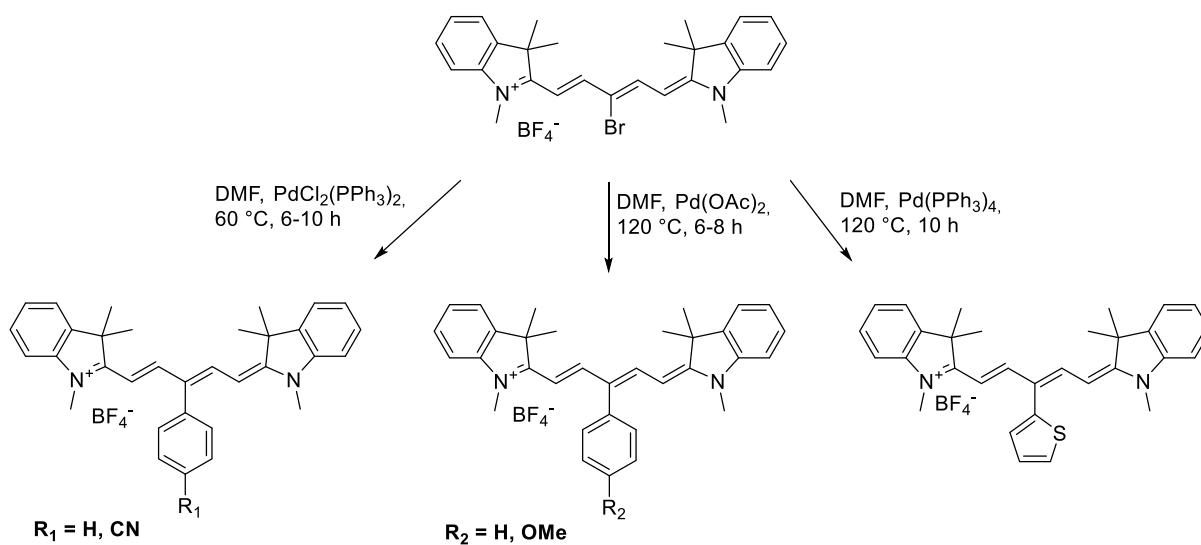


**Figure 13.** Palladium-catalyzed cross couplings of bromo-substituted pentamethines.

Heptamethine dyes containing rigid cyclohexene moieties are easily modified by nucleophilic substitution via a radical-nucleophilic aromatic ( $S_{RN}1$ ) mechanism.<sup>[30,45]</sup> The central chlorine atom is efficiently substituted by nucleophiles as thiols, phenolates and amines (see Figure 14).<sup>[46-48]</sup> Moreover, further functionalization provided NIR dyes with reactive functional groups such as NHS ester or isothiocyanates for subsequent coupling to biomolecules.<sup>[45,49]</sup>

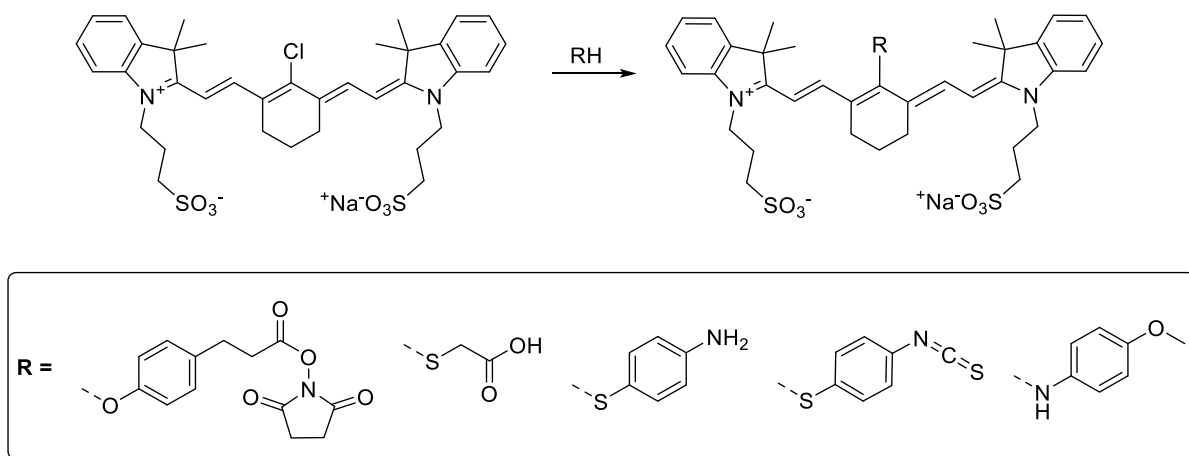


**Figure 14.** Nucleophilic substitution of the chlorine atom by thiols or phenolates.

Furthermore, the central chlorine atom was also replaced by a robust C-C bond via a palladium-catalyzed cross coupling. Chloro-substituted compounds are generally inert to oxidative addition of palladium-(0) complex in comparison to bromo or iodo derivatives.<sup>[50]</sup> However, Achilefu and coworkers presented the successful synthesis of aminophenyl-, hydroxyphenyl-, and carboxyphenyl-substituted heptamethine dyes via Suzuki-Miyaura coupling (see Figure 15).<sup>[51-52]</sup> More recently, bromo-substituted pentamethines were also successfully employed in Suzuki coupling to achieve stable C-C bonds.<sup>[53]</sup>

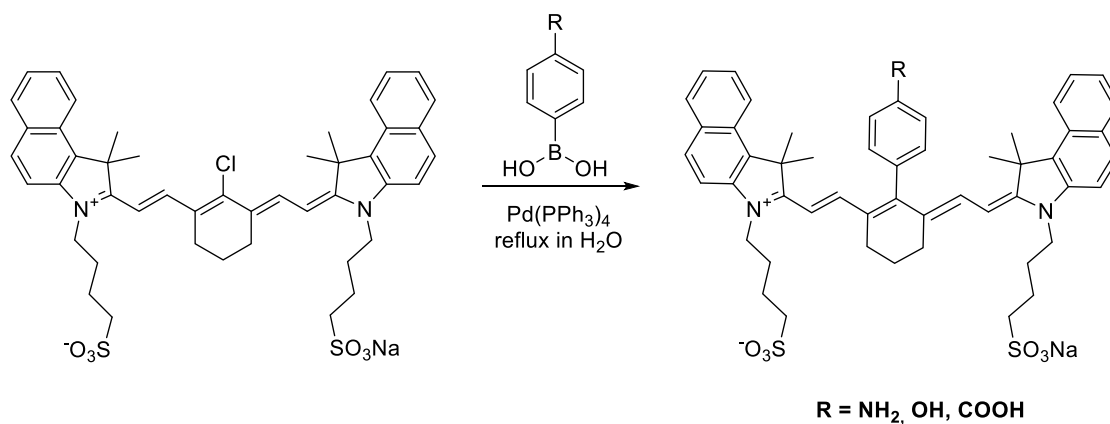


**Figure 15.** Suzuki reaction of chloro-substituted heptamethine dyes.

### (b) Aromatic System

Cyanine dyes without any aromatic substitutions cannot be modified any further and the introduction of reactive groups must be achieved before the indolenine formation. Aromatic positions of indolenines are usually equipped with sulfonic acid, since they are inert during dye

synthesis and they enhance the water solubility due to electrostatic repulsion, which is mandatory for biomedical applications. Common sulfo-substituted indolenines are portrayed in Figure 16 revealing the typical positions for indolenines on C-2 or C-1 and C-3. Waggoner et al. presented a sufficient route to sulfonated indolenines via conventional Fisher indole synthesis.<sup>[38-39,54]</sup> Indolenines were prepared from sulfo-substituted hydrazinobenzene and methyl isopropyl ketone in high yields of 73% (see Figure 16). In 1996, in the same laboratory, sulfonated benzindolenines were prepared from sulfonated naphthylamines and applied in further dye synthesis bearing up to four sulfonic acid groups.<sup>[39]</sup> Previous studies focused exclusively on the direct sulfonation of benzindolenines resulting in different orientations of the sulfonate groups.<sup>[55]</sup>

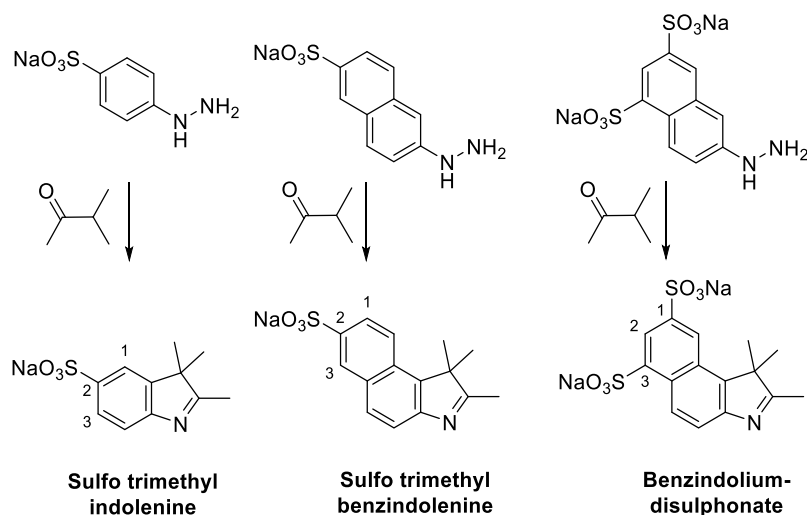


**Figure 16.** Synthesis of sulfonated trimethylindolenine and trimethylbenzindolenine derivatives from substituted hydrazinobenzene derivatives via Fisher indole synthesis.

Further derivatization of trimethylindolenines achieved the functionalized indoles illustrated in Figure 17 including carboxylic acids, nitro and amino groups directly attached to the aromatic system.<sup>[36,56-57]</sup> Furthermore, carboxyl and amino benzyl indolenine derivatives have been reported.<sup>[23,37,58-59]</sup>

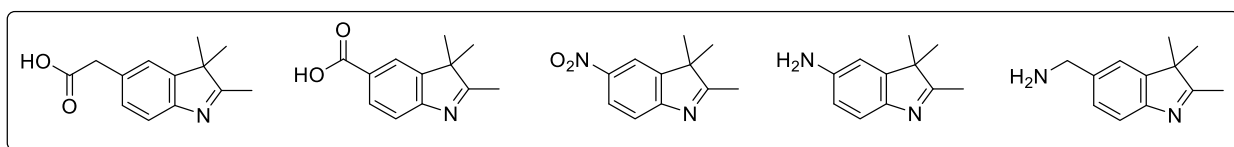


**Figure 17.** Trimethylindolenines with different aromatic substitutions.

### (c) Substituents at the indole nitrogen

Alkylation of nitrogen atoms in the heterocyclic system is carried out by nucleophilic substitutions of halogenalkanes. Historically indolenines were alkylated with short halogenated alkanes such as methyl iodide, but the resulting polymethine dyes were rather unpolar. To increase water solubility, Ernst and coworkers studied the incorporation of alkyl-sulfonates in dye structures. Nucleophilic substitution of 1,4-butanediol sulfonate provided indolenines alkylated with sulfobutyl chains.<sup>[23,36]</sup> Moreover, reaction of indolenine with bromohexanoic acid yielded dye structures with a functional group for further activation to NHS ester and bioconjugation.<sup>[38]</sup> Nitrogen alkylations are illustrated in Figure 18 including a new synthetic route to amino terminated indolenines. Romieu and coworkers presented the reaction of benzindolenines with (4-bromobutyl) phthalimide affording quaternary salts in high yields. Moreover, condensation with a carboxylated benzindolenine and subsequent deprotection with hydrazine yielded a cyanine-based amino acid.<sup>[60]</sup>

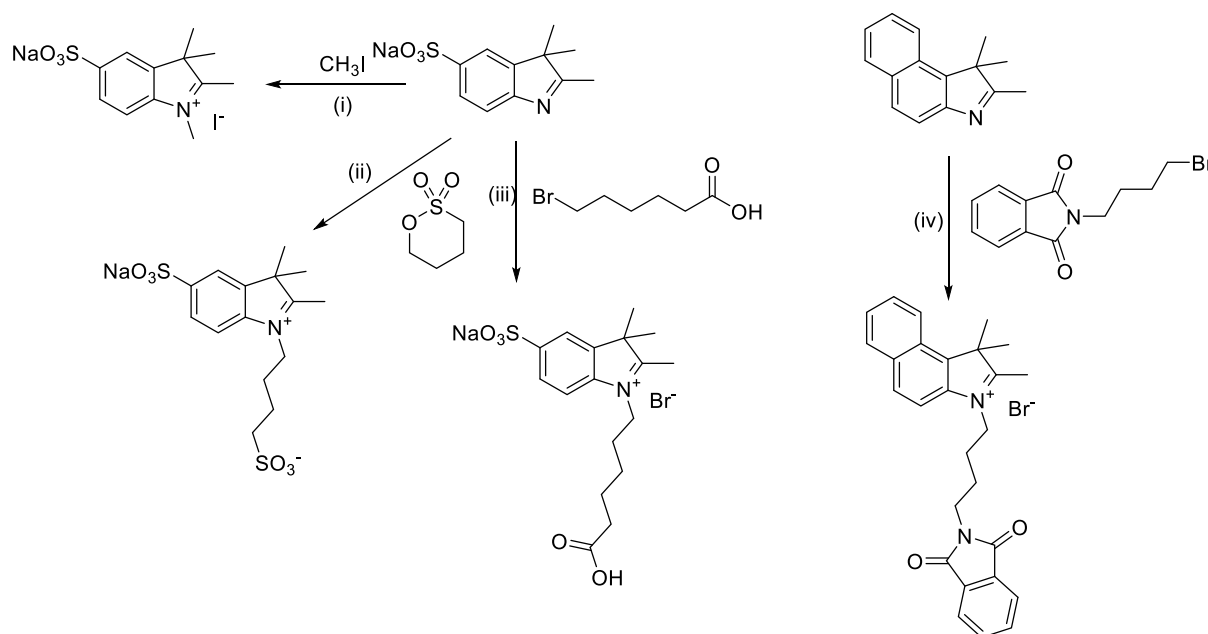


**Figure 18.** Nitrogen alkylation of sulfonated trimethylindoleine with (i) methyl iodide, reflux, 24 h, (ii) 1,4-butane sultone, 1,2-dichloro benzene, 110 °C, 12 h, or (iii) 6-bromohexanoic acid, 1,2-dichloro benzene, 110 °C, 12 h and benzindolenine alkylated with (iv) (4-bromobutyl)phthalimide, 140 °C and subsequent deprotection with hydrazine, methanol, and chloroform.<sup>[38,60]</sup>

### 1.3.4 Optical Properties and Aggregation Behavior

Cyanine dyes are broadly applied in biomedical imaging since virtually any desired wavelength from the visible (VIS) and NIR light can be achieved. Moreover, their color is strongly

influenced by the length of the conjugated system, which can be extended by the elongation of the polymethine chain and furthermore adjusted by the substitution of the terminal heteroaromatic structure. With each step of extending the polymethine chain by one methine group (CH=CH), the absorption maximum is red-shifted by approximately 100 nm.<sup>[31]</sup> Moreover, the bathochromicity is strongly influenced by the electron-releasing power of the donor nitrogen, which is preferably enclosed in a heterocyclic system. Generally, cyanine dyes exhibit narrow absorption bandwidths (for organic dyes) and are exceptionally bright. Narrow bandwidths are characterized by a close geometry of first excited state and the ground state, and for cyanine dyes they are very similar.<sup>[20,26]</sup> Figure 19 illustrates the typical spectra of three indocarbocyanine dyes ( $n = 1, 2, 3$ ) revealing their narrow and mirror-like absorption and emission peaks.

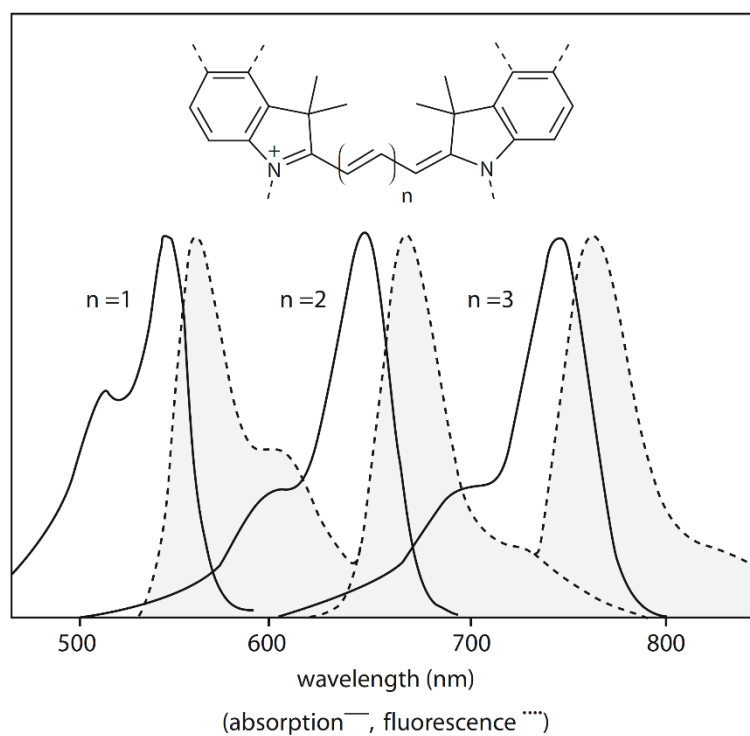


**Figure 19.** Absorption and emission spectra of carbocyanines dyes ranging from ICC ( $n = 1$ ) to ITCC ( $n = 3$ ). Adapted with permission from Klohs et al.<sup>[61]</sup>

The color strength of cyanine dyes is based on their highly allowed HOMO to LUMO transition resulting in high  $\epsilon$  values in the range of 50,000 to 250,000  $\text{L} \cdot \text{mol}^{-1} \cdot \text{cm}^{-1}$ .<sup>[26]</sup> The characteristic shoulder at smaller wavelengths ascends from vibrational transitions of the first excited state.<sup>[62]</sup> Furthermore, the energy difference between the absorbed and emitted photon, the Stokes shift, for cyanine dyes is rather small as usually observed for long-wavelength fluorophores.<sup>[63]</sup> Cyanine dyes exhibit rather small fluorescence quantum yields  $\phi_f$  of up to 30%, but as



mentioned before are rather insensitive to solvent polarity.<sup>[6,64]</sup> The influence of the polymethine chain length is illustrated in Figure 20 showing the characteristic peak shift of 100 nm with increasing chain length. Moreover, trimethines reveal smaller fluorescence quantum yields than penta- and heptamethines, and higher molar absorption coefficients are also achieved for red-shifted dyes.<sup>[38]</sup>

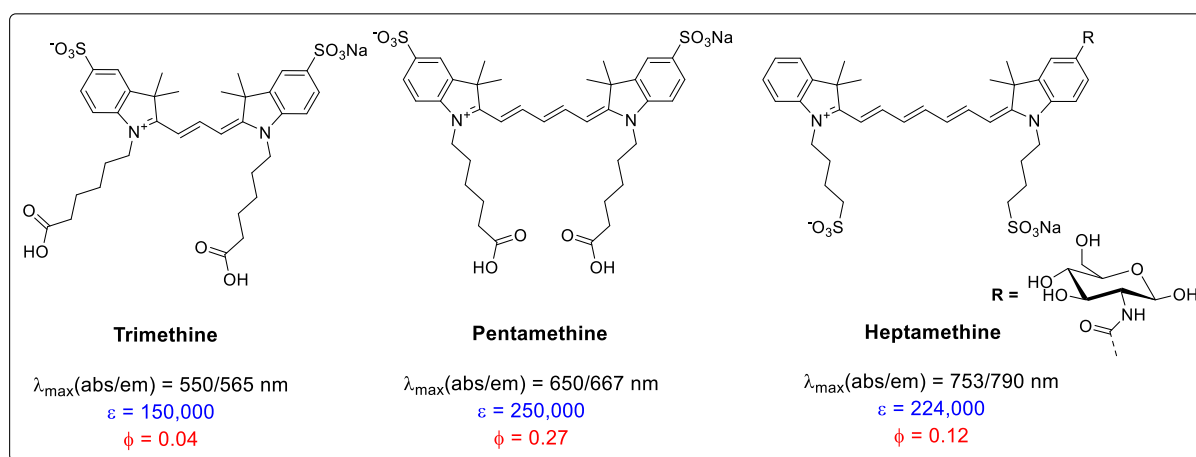


**Figure 20.** Optical properties of sulfo-cyanines of varying polymethine lengths measured in PBS solution.<sup>[38]</sup>

There are several options to tune optical properties of cyanine dyes. For example, binding to proteins or nucleic acids increases the fluorescence emission due to rigidization of the chromophore.<sup>[65-67]</sup> Hence, an important aspect influencing the optical properties is derived from their interaction with binding partners, or their ability to exert self-assembly and aggregation.

Cyanine dyes are well known to form self-assembled aggregates depending on the dyes' orientation to each other and their dipole moments. Aggregation formation strongly effects absorbance and fluorescence of the dyes leading to shifted peaks and decreased fluorescence quantum yields. Generally, aggregates are differentiated in H-aggregates versus J-aggregates.<sup>[68]</sup> H-type aggregates are characterized by a blue-shifted (hypsochromic) absorption band forming sandwich-type aggregates in a plane-to-plane stacking. In contrast, J-type aggregates orientate in head-to-tail arrangement (end-to-end stacking) resulting in red-shifted (bathochromic) peaks as shown in Figure 21.<sup>[69]</sup> While H-aggregates reveal broad peaks and negligible fluorescence, J-aggregates are distinguished by a narrow band and reveal enhanced fluorescence.<sup>[6,70]</sup>

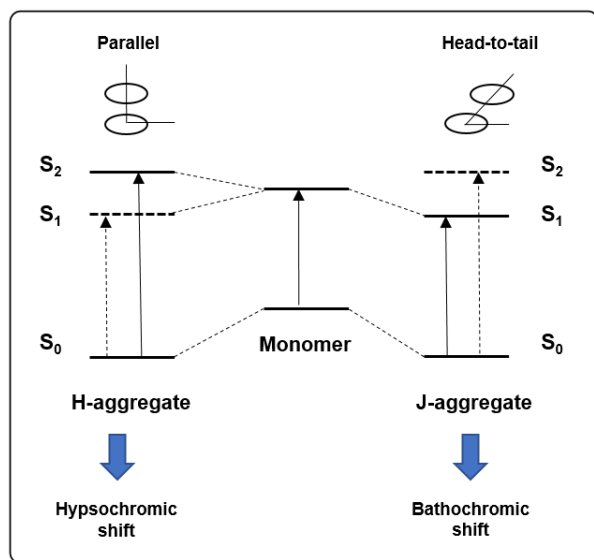


**Figure 21.** Schematic presentation of the relationship between electronic transition, spectroscopic shift and the arrangement of molecules in H- and J-aggregates.<sup>[68]</sup>

There is a strong interdependency of aggregation properties and states, and the resulting photostability is strongly influenced by structural modifications. Introduction of several groups to reduce the formation of aggregates also improves photostability as aggregated states are known to degrade in the presence of light and molecular oxygen.<sup>[29]</sup> Compared to other heterocyclic substitutions, indocarbocyanine dyes exhibit higher photostability.<sup>[29]</sup> While terminal substitutions of the heterocycle such as benzene moieties only effect the photostability minorly,<sup>[27]</sup> fluorinated thiocyanines have shown improved resistance in photobleaching.<sup>[71]</sup> The polymethine chain length has a strong effect though and the increasing chain length causes a decrease in stability of the chromophore. Cyanine dyes are much more stable in polar solutions, because the rate of photooxidation is reduced due to less formation of singlet oxygen.<sup>[27,72]</sup> Photodegradation is caused by an interaction between the triplet state of the dye and triplet oxygen  $^3\text{O}_2$  inducing the singlet oxygen  $^1\text{O}_2$ . Subsequently, the polymethine chain is attacked by  $^1\text{O}_2$  resulting in photooxidation and fragmentation of the chromophore as illustrated in Figure 22.<sup>[14,29]</sup>

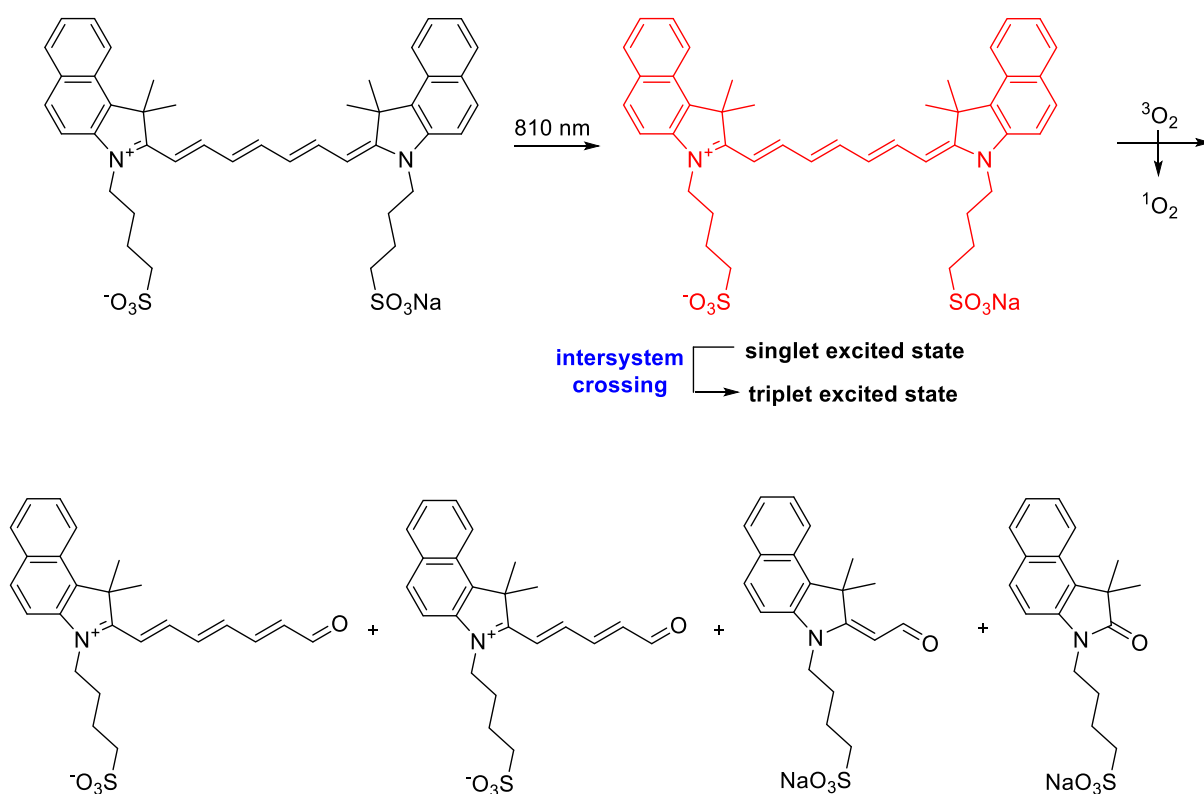


**Figure 22.** Mechanism of photodegradation of a heptamethine by singlet oxygen.<sup>[14]</sup>

To overcome unfavorable aggregation, structural modifications of cyanine dyes have been attempted including steric protection, electronic effects, or electrostatic repulsion. In 1997 Guether et al. analyzed cyanine- $\beta$ -cyclodextrin derivatives and observed enhanced photostability of the fluorophore.<sup>[73]</sup> The formation of an inclusion complex between chromophore and cyclodextrin inhibits the photodegradation of the dye. Furthermore, photostability can be enhanced by suppressing aggregation and introducing sterically bulky groups. For example, dimethylindolium dyes are less prone to photodegradation than benzothiazolium or benzoxazolium dyes due to unfavorable steric interactions of the dyes.<sup>[29]</sup> Chen et al. characterized benzene-N-alkylated heptamethines and compared the influence of different substituents on the photostability.<sup>[74]</sup> Furthermore, the incorporation of fluorine atoms on the heterocyclic system was reported to reduce photobleaching and suppress aggregation in aqueous media.<sup>[71]</sup> Additionally the dye exhibited enhanced fluorescence quantum yields and was less sensitive to singlet oxygen. As discussed in the previous chapter, anionic groups such as sulfonic acid were introduced to add water solubility, but they also prevent intermolecular interactions by shielding the chromophore. Sulfonic acid can be attached as alkylsulfonates affixed to the nitrogen atoms or on the benzene moieties. In 2013, Resch-Genger et al. presented

a new benzindocyanine incorporated with a maximum of six sulfonic acids to tune spectroscopic properties by efficiently suppressing aggregation.<sup>[53]</sup> By rigidization, photostability of cyanine dyes can be enhanced by inhibiting radiationless internal conversions and subsequent isomerization.<sup>[29-30,75-77]</sup> Rigidization in heptamethine dyes is usually done by introducing a ring system into the polymethine chain as already mentioned in the previous chapter. Chemical structures of the modifications described here are illustrated in Figure 23.

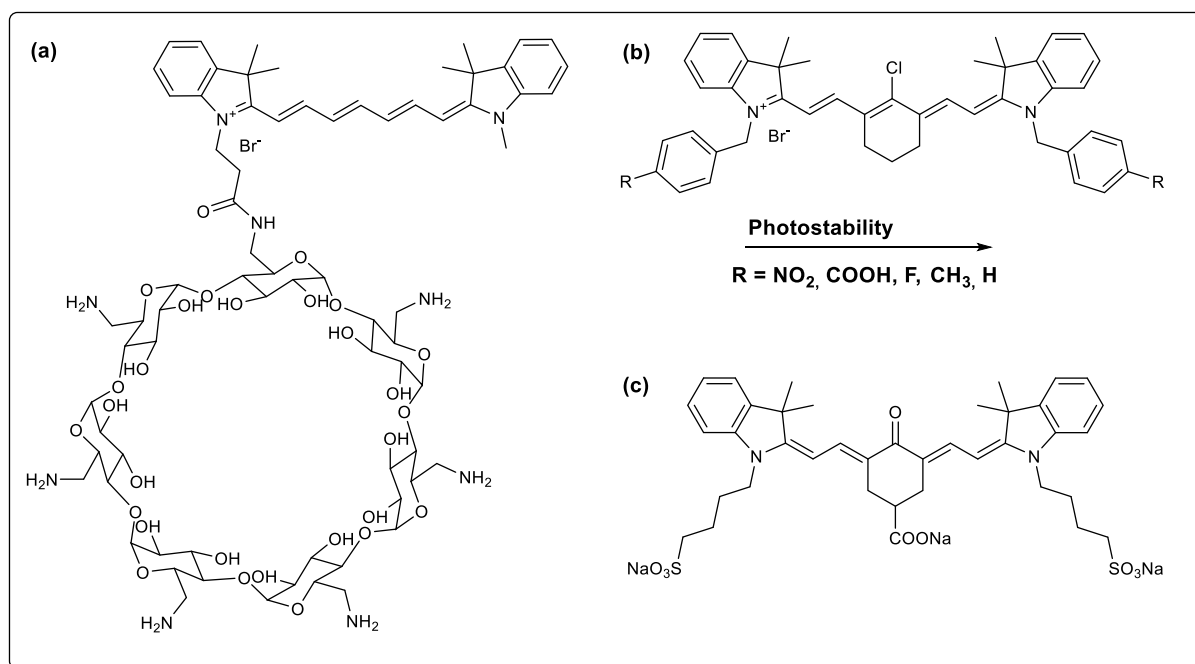


**Figure 23.** Enhancement of photostability by the introduction of  $\beta$ -cyclodextrins (a),<sup>[73]</sup> N-alkylation with bulky benzene residues (b)<sup>[74]</sup> and incorporation of six sulfonic acids (c).<sup>[77]</sup>

The suppression of aggregation is one of the key approaches for the enhancement of optical properties, which can be realized by systematically modifying different positions in the chromophore. As previously discussed, three positions are available: the *meso*-position of the polymethine chain, the aromatic system, and the nitrogen atoms terminating the polymethine chain. Substitution at the *meso*-position influences the molar absorption coefficient. Generally, *meso*-alkylated cyanine dyes, at least those with aliphatic substituents, exhibit smaller coefficients than non-substituted dyes due to destabilization of *trans*-isomers.<sup>[62,78]</sup> Optical properties of *meso*-substituted pentamethine dyes illustrated in Figure 24 reveal a decrease in fluorescence quantum yield for any substitution (electron-withdrawing or alkyl), but molar absorption coefficients increase upon modification of the *meso*-position.<sup>[53,79]</sup>

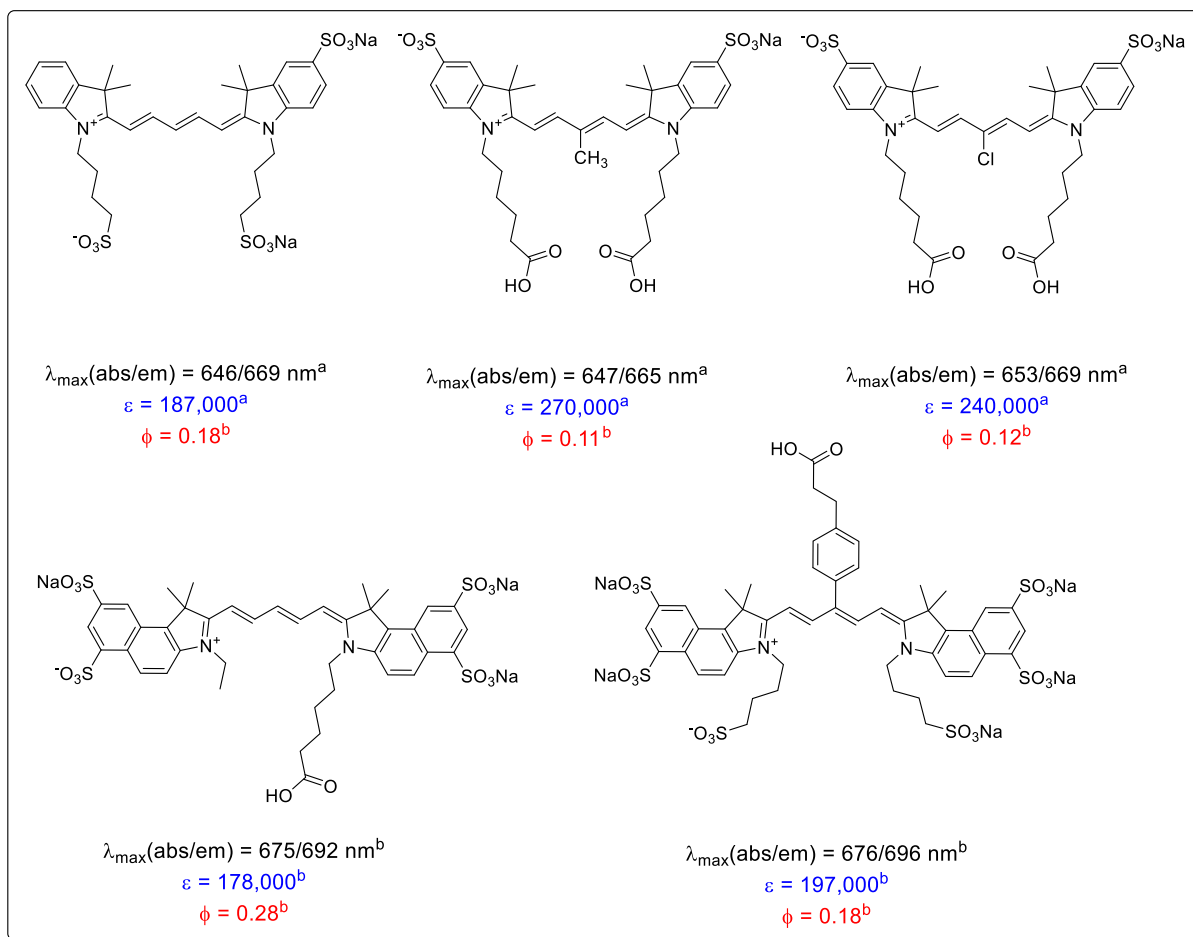


**Figure 24.** Optical properties of *meso*-substituted dyes compared to non-substituted cyanine dyes (<sup>a</sup>PBS, <sup>b</sup>methanol).<sup>[53,79]</sup>

In 2005, Peng and coworkers showed the synthesis of heptamethine with robust C-N bonds which strongly influenced optical properties due to the direct involvement of nitrogen electron pairs.<sup>[80]</sup> Chloro-substituted heptamethine dyes were reacted with primary amines substituting the chlorine by an  $S_{\text{RN}}1$  pathway, as illustrated in Figure 25. They reported a large Stokes shift of about 150 nm and a considerable enhancement of fluorescence quantum yields up to 47%. Absorption and emission spectra were broadened, blue-shifted ( $\sim 180$  nm) and appeared less defined without the typical mirror-image relationship. As a shift in absorption spectra with increasing solvent polarity was observed, the authors proposed an excited-state intramolecular charge transfer (ICT), which is typically accompanied with a solvatochromism.<sup>[81]</sup> Substitution patterns of the aromatic system also strongly influence the spectroscopic properties, particularly when aggregation is reduced.

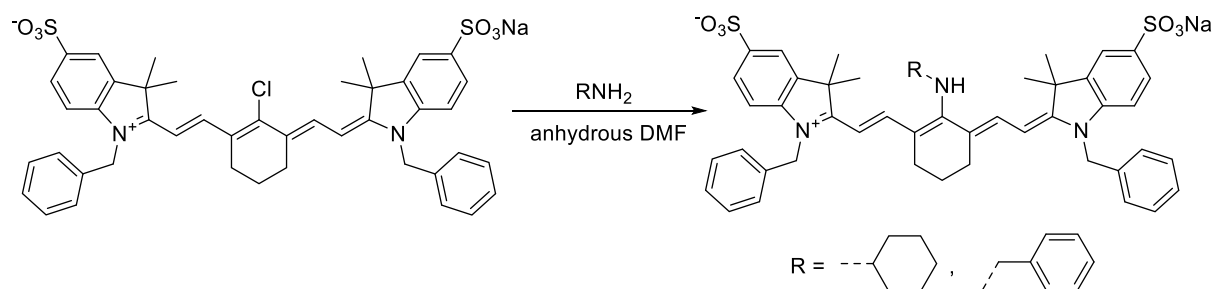


**Figure 25.** Nucleophilic substitution of heptamethine dyes via a  $S_{\text{RN}}1$  mechanism.<sup>[80]</sup>

Figure 26 illustrates the clinically approved dye ICG exhibiting low quantum yields (1%) and strongly enhanced quantum yield values (up to 12%) when attaching glucosamides to the heterocyclic system of heptamethines.<sup>[57]</sup> Moreover, the molar absorption coefficients are increased additionally resulting in increased brightness. Mujumdar and coworkers studied the influence of sulfonic acids on benzindolenines revealing a strong increase in  $\phi_f$  values when incorporating four sulfonic acid groups instead of two to the chromophore.

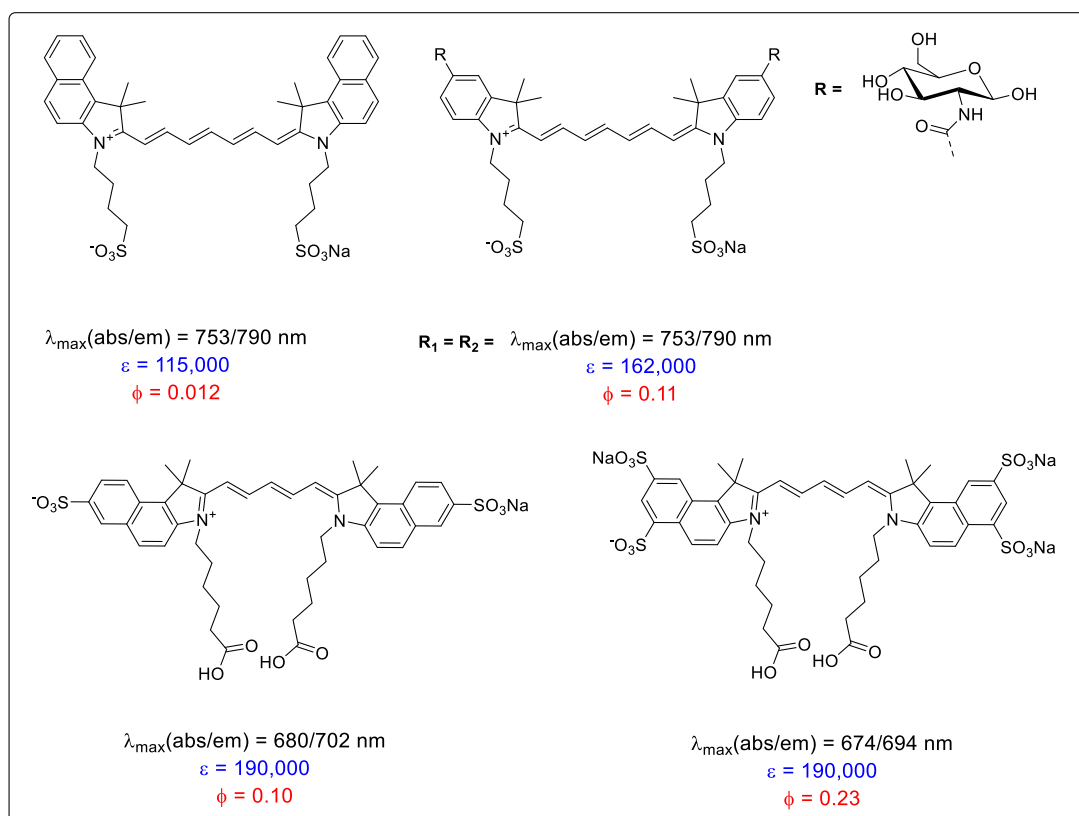


**Figure 26.** Influence of aromatic substitution by the introduction of sugar moieties<sup>[57]</sup> or sulfonic acids<sup>[39]</sup> on the heterocyclic system.

While the influence of nitrogen substituents is not as pronounced as the other position, they still have an influence on the photostability. However, benzyl substituents have shown a slight

enhancement of molar absorption coefficients when compared to alkylated nitrogen atoms in heptamethine dyes (see Figure 27).<sup>[48,74]</sup>

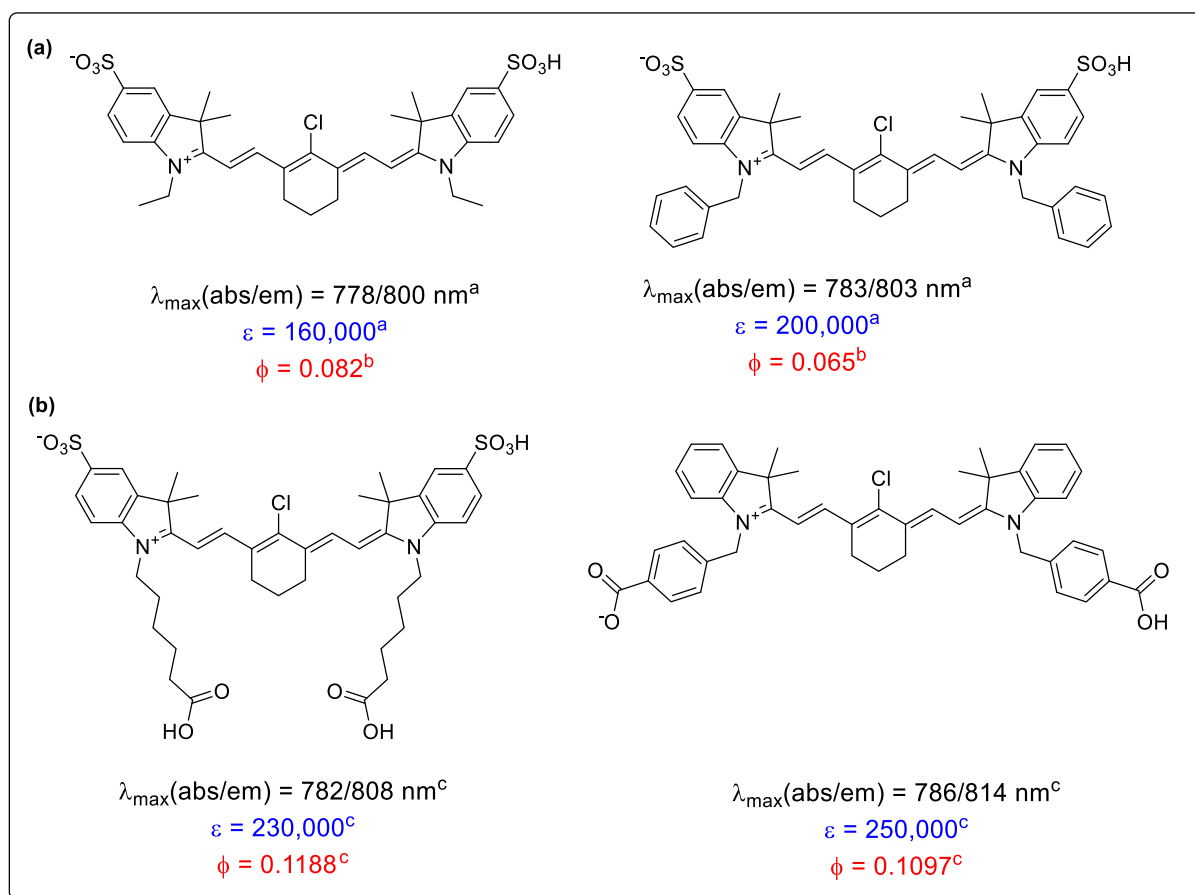


**Figure 27.** Influence on spectroscopic data (<sup>a</sup>water, <sup>b</sup>DMSO, <sup>c</sup>methanol) of alkyl- vs. benzyl-substituted nitrogen (a) without benzene substitution and (b) with terminal carboxylic acids.

### 1.3.5 Responsive Cyanine Dyes

Responsive probes are equipped with a functionality that is sensitive to environmental changes resulting in change of the fluorescence properties. Furthermore, these external stimuli must be reversible such as pH change or protein binding. In the literature, two types of pH-sensitive cyanine dyes are described: one of them features non-N-alkylated indolenines, while the other one is based on photoinduced electron transfer (PeT).<sup>[82]</sup> The first type of pH-sensitive cyanine dyes is characterized by a non-alkylated nitrogen atom at one of the indolenines generating highly fluorescent dyes upon protonation. Generally, deprotonation leads to disruption of the characteristic resonance structure of cyanine dyes and leads to a non-fluorescent base form (shown in Figure 28).<sup>[83]</sup>

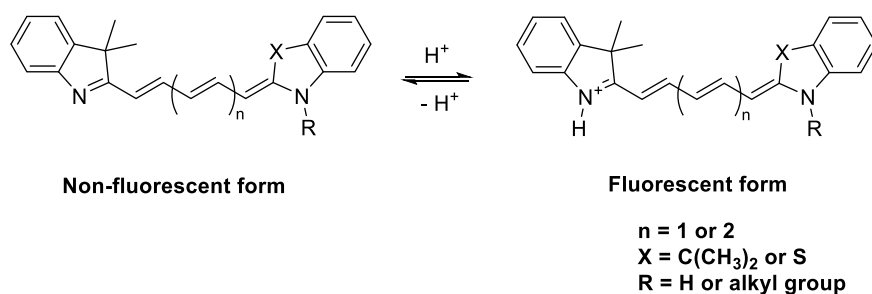


**Figure 28.** pH-sensitive cyanine dyes based on non-alkylated nitrogen atoms.

In the past years, several pH-sensitive dyes based on non-N-alkylation have been synthesized,<sup>[84-88]</sup> but only a few samples reveal  $pK_a$  values close to physiological conditions ( $\text{pH} < 7$ ). Among them is a substituted pentamethine with sulfonic acids to improve water solubility revealing  $pK_a$  values of 6.2 (see Figure 29).<sup>[89]</sup> Moreover, the pH-sensitive dye was also incorporated in perfluorocarbon nanoemulsions for the intracellular pH measurement. By combining a pH-sensitive (CypHer5) and non-pH-sensitive dye (Cy3), Waggoner et al. performed ratiometric measurements for the determination of absolute pH values from a calibration curve.<sup>[90]</sup>

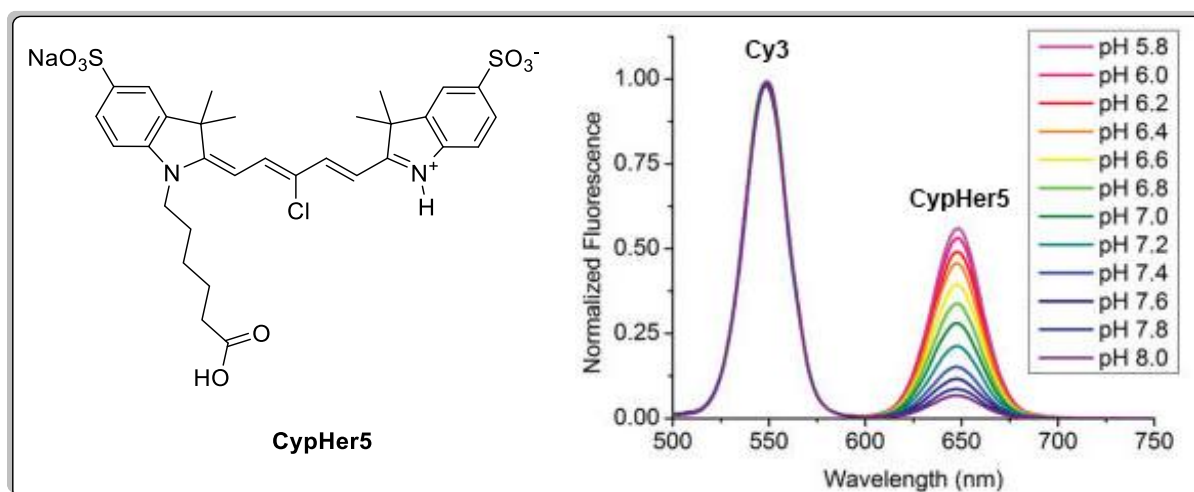


**Figure 29.** Protonated structure of CypHer5 and absorption spectra of a nanoformulation with conjugated pH-insensitive dye (Cy3) and pH-sensitive dye (CypHer5). Adapted with permission from Patrick et al.<sup>[90]</sup> Copyright 2013 American Chemical Society.

pH-sensitive dyes based on PeT processes consist of a cyclohexyl-bridged heptamethine with a nitrogen-modulator.<sup>[82]</sup> Fluorescence tuning is achieved by turning the PeT on or off due to



protonation or deprotonation of the modulator. At high pH values the PeT process is quenched which leads to low emission. Upon acidification, the nitrogen atom hampers the PeT process which leads to bright fluorescence. Figure 30 illustrates the process and shows two examples from the literature, which are both cell permeable. Via nucleophilic substitution, *meso*-substituted heptamethine dyes were generated for which  $pK_a$  values of 7.1 and 5.1 were achieved.<sup>[91-92]</sup> Upon protonation, the aminophenol-substituted derivative even reveals a 10-fold enhance of fluorescence intensity.<sup>[91]</sup>

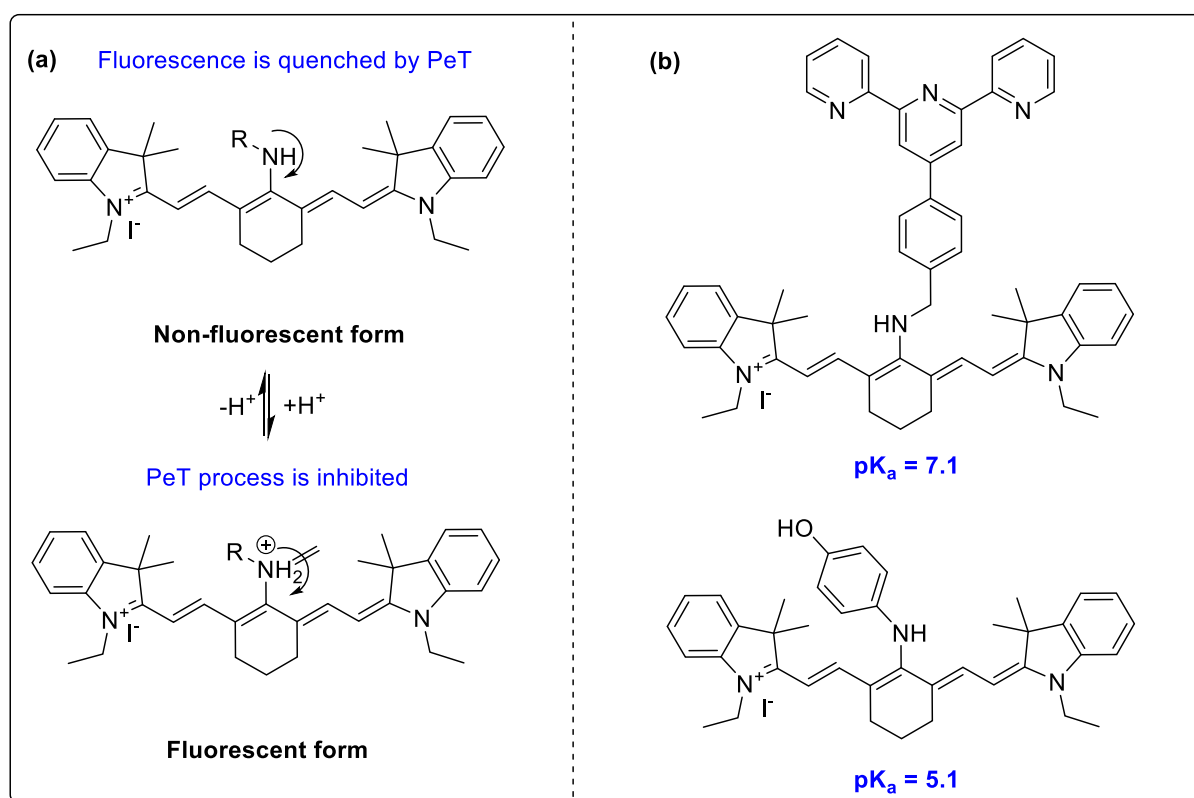


**Figure 30.** (a) Photoinduced-electron transfer (PeT) process and (b) two examples for N-substituted heptamethine dyes.<sup>[82,91-92]</sup>

Another approach to achieve responsive probes is to enhance the fluorescence emission by binding a certain moiety due to aggregate dissociation. In 2005, Patonay et al. reported the synthesis of bis(heptacyanines) which consists of two heptamethine dyes bridged through an alkyl spacer of differing lengths ( $n = 4, 6, 8, 10$ ) shown in Figure 31.<sup>[93-94]</sup> The biscyanines assemble in strong H-aggregates and reveal low molar absorption coefficients and fluorescence quantum yields due to inter- and intramolecular interactions. Upon binding to human serum albumin (HSA), an emission is observed as H-aggregates open up and the strongest enhancement was observed for derivatives with four methylene groups.

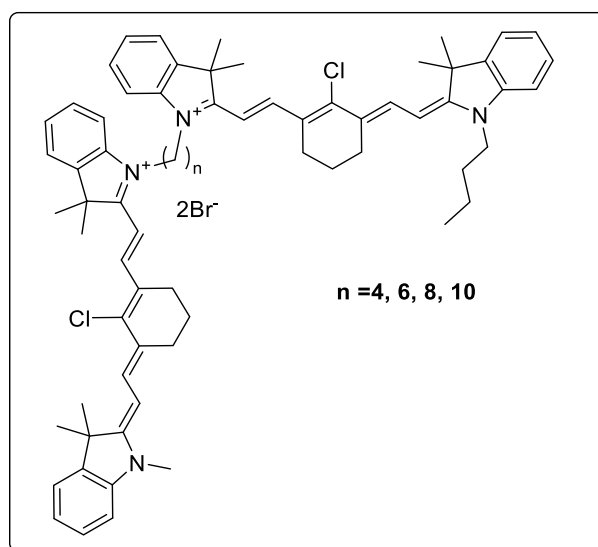


**Figure 31.** Structure of two heptamethine dyes connected via an alkyl spacer with varying lengths.

### 1.3.6 Activatable Probes based on Cyanines

Activatable probes are characterized by a non-emitting fluorophore that is either connected to a cleavable linker or transformed by chemical modification of the  $\pi$ -system. In response to environmental changes, the emission is selectively switched on, but in contrast to responsive sensor dyes this process is irreversible.

Cleavable probes are typically attached to a carrier (protein or polymer backbone) and contain one or two fluorophores that form non-emissive aggregates. Upon cleavage by enzyme activity, pH change, or oxidation, the dye is released and the initially quenched fluorescence is restored. Weissleder and coworkers created an enzyme-cleavable fluorescence probe which becomes highly emissive upon cathepsin D cleavage.<sup>[95]</sup> A pentamethine dye was attached to an 11 amino acid peptide with specificity for cathepsin D, an enzyme which is overexpressed in many tumors. *In vitro* studies of the probe, which was immobilized on a polymer backbone, confirmed the enzyme activity by revealing a 350-fold signal enhancement of the cleaved cyanine dye relative to its carrier-bound state. A broad variety of approaches based on cleavable peptide substrates, either on polymer carriers or as smaller entities with dimeric dyes attached, have been reported.<sup>[96-99]</sup>

Another more elegant approach for organic chemists involves the design of activatable probes which exhibit a sensor function built into the chemical structure of the  $\pi$ -system of the polymethine chain itself. This is achieved by the incorporation of specific moieties which

undergo a reorganization of a previously disturbed  $\pi$ -system thereby creating the emissive fluorophore structure upon a certain cleavage of trigger process. By the incorporation of an aromatic ring into the polymethine chain, Shabat and coworkers introduced new NIR fluorophores with a tunable emission.<sup>[100]</sup> In contrast to conventional cyanine dyes, the incorporated phenol leads to positive charges on both nitrogen atoms resulting in a different conjugation pattern and low absorption. Upon deprotonation, a quinone is generated by mesomerization of the phenol form, which results in significant fluorescence emission (Figure 32). By converting the phenol group into an ether, the fluorophore is trapped in its non-fluorescent form. The authors describe the introduction of a phenyl boronic acid via substitution and subsequent dye formation yielding a non-fluorescent probe. Unmasking the probe by oxidation of phenylboronic acid followed by hydrolysis and elimination of p-quinone-methide leads to the release of a strong NIR-emitting fluorophore.

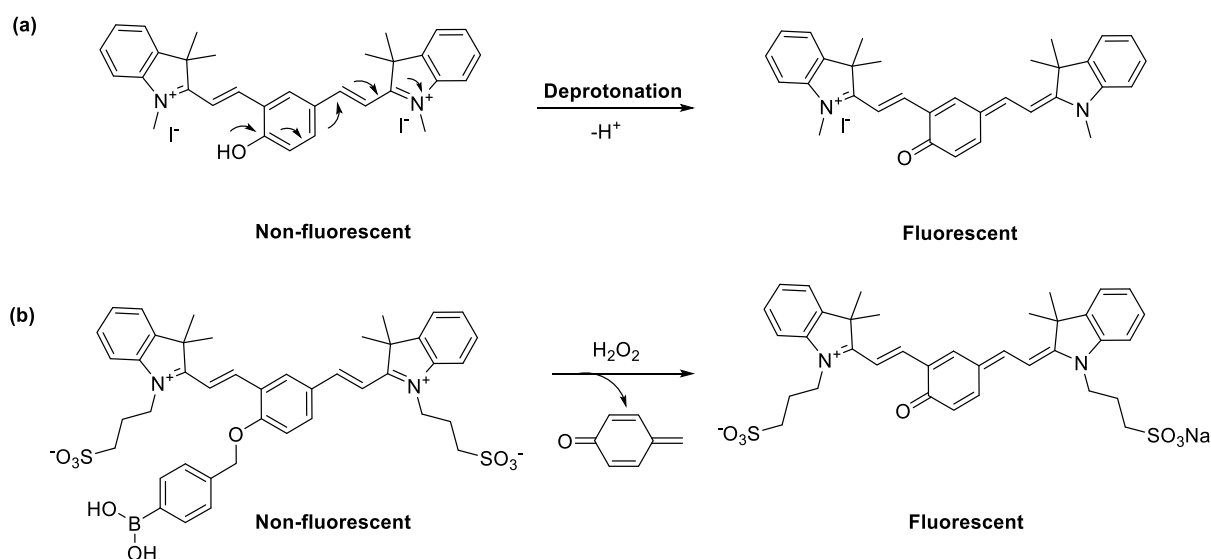


**Figure 32.** NIR fluorophores, which transform from phenol form into a quinone upon deprotonation (a), and reaction with H<sub>2</sub>O<sub>2</sub>, which restores the quinone derivative (b).<sup>[100]</sup>

Based on these turn-On NIR cyanine dyes they developed several probes for the detection of specific analytes including hydrogen peroxide, thiols and  $\beta$ -galactosidase.<sup>[101]</sup> They described the synthesis of NIR dyes equipped with  $\beta$ -galactose and the fluorescence enhancement upon reaction with  $\beta$ -galactosidase (see Figure 33). *In vivo* studies revealed a high signal-to-noise ratio for injected probes only when the analyte was co-injected. Furthermore, in 2015, they also reported the synthesis of a turn-On NIR dye containing phenyl boronic acid as detection unit and camptothecin as an inactivated drug.<sup>[102]</sup> Upon reaction with hydrogen peroxide, the dye is turned on and releases the active drug through an self-immolative linker.

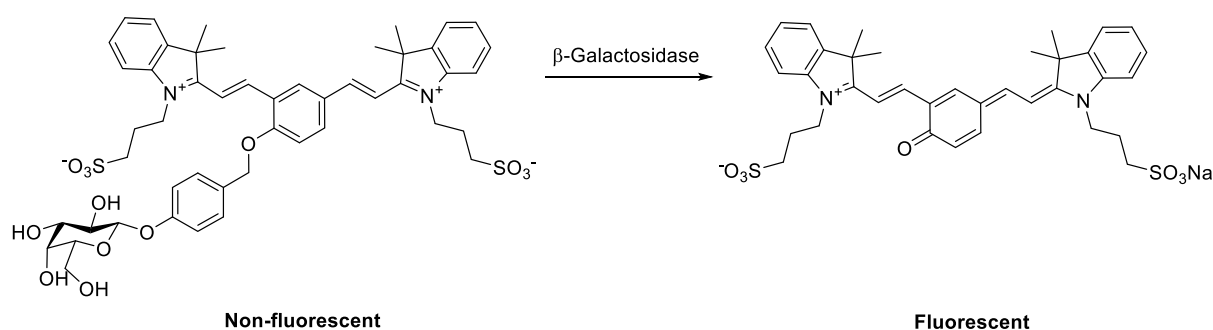


**Figure 33.** Cleavage of O-glycosidic bond on a turn-On heptamethine upon reaction with  $\beta$ -galactosidase.<sup>[101]</sup>

As opposed to the deactivated fluorophores synthesized by Shabat et al., in 2009 another approach towards reduced cyanine dyes was reported by using reactive oxygen species (ROS) for oxidation. The term ROS summarizes several oxygen radicals such as hydrogen peroxide ( $\text{H}_2\text{O}_2$ ), hydroxyl radical ( $\text{HO}^\cdot$ ) and superoxide anion ( $\text{O}_2^-$ ) which are generally produced in the normal cell metabolism.<sup>[103]</sup> However, altered levels result in oxidative stress which is linked to several diseases such as cardiovascular diseases, cancer, and neurological disorders.<sup>[104-107]</sup> Kundu et al. reported in 2009 a facile approach for generating ROS sensors from commercially available cyanine dyes.<sup>[108]</sup> These hydrocyanines are prepared by the reduction of the iminium cations with sodium borohydride and are weakly fluorescent due to the disruption of the  $\pi$ -system. Upon oxidation with superoxide or hydroxyl radicals, their fluorescence is regenerated and dramatically increased by a 100-fold increase (see Figure 34).

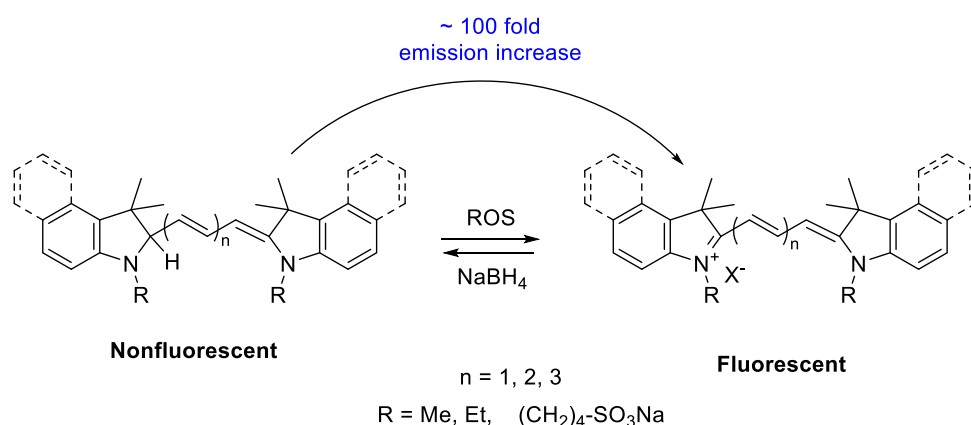


**Figure 34.** Oxidation of hydrocyanines to highly fluorescent cyanine dyes by ROS.

Subsequent cell and *in vivo* studies revealed successful ROS detection of angiotensin-mediated and lipopolysaccharide (LPS) endotoxin-induced oxidative stress. Based on these findings,

further studies described the imaging of implant-associated inflammation and tumor-inflammation site using hydrocyanine-conjugated nanocarriers.<sup>[109-110]</sup>

In 2010, Nagano and coworkers studied the sensitivity of cyanine dyes towards ROS and reported a higher stability against radicals for pentamethine derivatives over NIR fluorophores.<sup>[111]</sup> For heptamethine dyes oxidation was observed as the polymethine chain degraded and yielded 1,3,3-trimethyloxindole. Moreover, they reported enhanced stability of sulfonated pentamethine dyes due to the electron-withdrawing group in contrast to heptamethine with thioether-substitution on the *meso*-position. Covalent linkage of both dyes led to dramatically quenched emission by a FRET mechanism. The oxidation by ROS led to degradation of the labile heptamethine and resulted in emission restorage of the pentamethine dye (see Figure 35), thus acting via the quenching and activation mechanism similar to the enzyme-activatable probes described above. Moreover, the conjugate successfully detected ROS production in cells and was applied for imaging oxidative stress in a peritonitis mouse model.

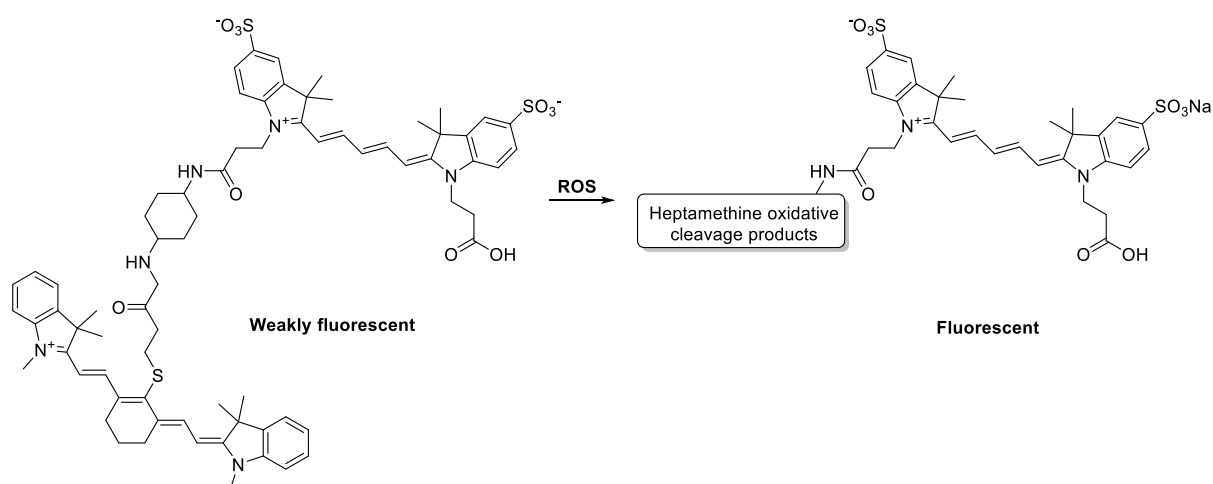


**Figure 35.** Covalent linkage of a pentamethine with a heptamethine dye and the subsequent oxidation resulting in fluorescent pentamethine dye.<sup>[111]</sup>

## 2 MOTIVATION AND OBJECTIVES

Cyanine dyes are broadly applied as labels for imaging probes due to versatile synthetic possibilities of adapting the fluorophore to the demands of labeling, targeting and imaging. By extending the polymethine chain almost every absorption wavelength within the visible and near infrared region can be accomplished making them applicable for superficial to deep tissue imaging.<sup>[6]</sup> However, cyanine dyes still suffer from several disadvantages, most importantly their low fluorescence quantum yield and high aggregation in aqueous solution as well as the general challenge to synthesize more sophisticated derivatives employing multifunctionality and capability to work as sensors.

Therefore, the goal of this work was the specific synthetic modulation of cyanine dyes by addressing three different positions in the chemical structure of the cyanine dye chromophore with the aim to generate highly fluorescent fluorophores with optimal water solubility and less tendency to form aggregates, synergistically combined with sophisticated sensor properties or reactive functionalities. The three main positions to effectively modify the cyanine dye structure and properties were (1) the substitution pattern at the heterocyclic nitrogen atoms, (2) the *meso*-position in the polymethine chain, and (3) the nature of the aromatic system including its residues.

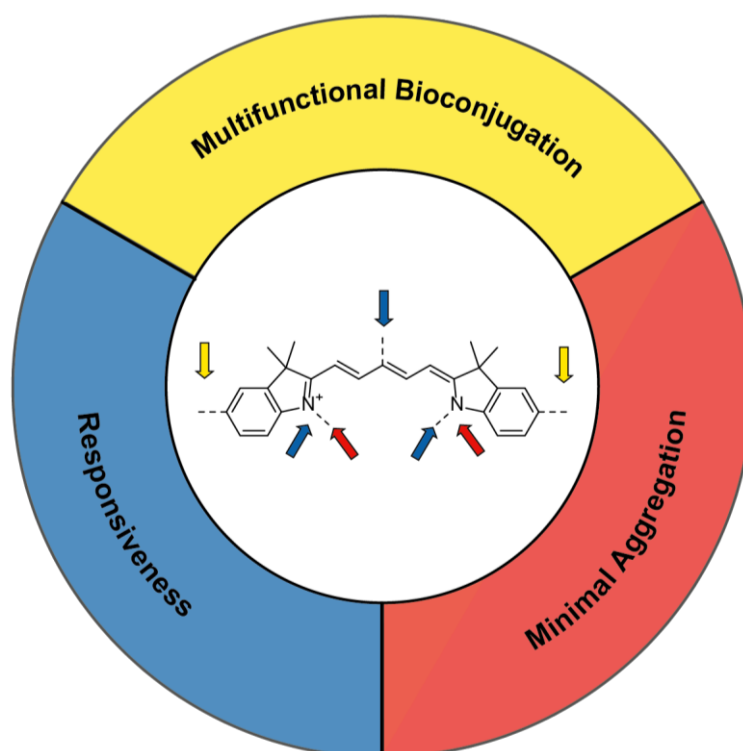


**Figure 36.** Illustration of cyanine modifications to yield dyes with responsive properties, reduced aggregation and with multifunctional properties.

The first objective was to increase water solubility and to minimize aggregation of the cyanine dyes. The goal was to apply glycerol-based dendron moieties and short PEG chains by attaching them covalently at the heterocyclic system by employing residues suited for nucleophilic substitution at the nitrogen atoms. Dendron moieties of varying generations have proven to increase water solubility on perylene dyes and moreover prevented them from aggregation by steric shielding<sup>[112-113]</sup>, but have not yet been applied for cyanine dyes.

In the second project, the focus was set on creating a pH-responsive dye which is achieved by non-alkylated heterocyclic nitrogen. Lessons learned from attempts to improve solubility were incorporated into the synthetic approach. Moreover, the *meso*-position in the polymethine chain was employed to study whether substituents are able to modulate the emission properties and dependency from pH in solution.

The objective of the third project was to create a novel cyanine structure capable to serve as a bifunctional and fluorescent linker between any desired type of biomolecule or polymer. To approach this goal, the aromatic positions of the heterocyclic system were used to generate a rigid and fluorescent linker. Therefore, different indolenine precursors were used to create a bifunctional asymmetric dye with two different reactive groups and good water solubility. The functional groups should be applicable in orthogonal labeling reactions. Linking or labeling of biomolecules usually requires mild reaction conditions, which should be considered when choosing the functionalities.

Therefore, the main objectives of this thesis were (1) incorporation of glycerol-based dendron moieties and PEG by N-substitution, (2) the synthesis and application of a responsive dye with tunable emission, and (3) establishment of a synthetic route to fluorescent heterobifunctional linkers based on cyanine dyes.

### 3 PUBLICATIONS AND MANUSCRIPTS

The following chapter lists all published articles as well as submitted manuscripts and highlights the author's contributions.

#### 3.1 Glycerol-Based Contrast Agents: A Novel Series of Dendronized Pentamethine Dyes

Virginia Wycisk, Jutta Pauli, Pia Welker, Aileen Justies, Ute Resch-Genger, Rainer Haag and Kai Licha\* *Bioconjugate Chemistry* **2015**, 26 (4), 773-781.<sup>[114]</sup>

<http://dx.doi.org/10.1021/acs.bioconjchem.5b00097>

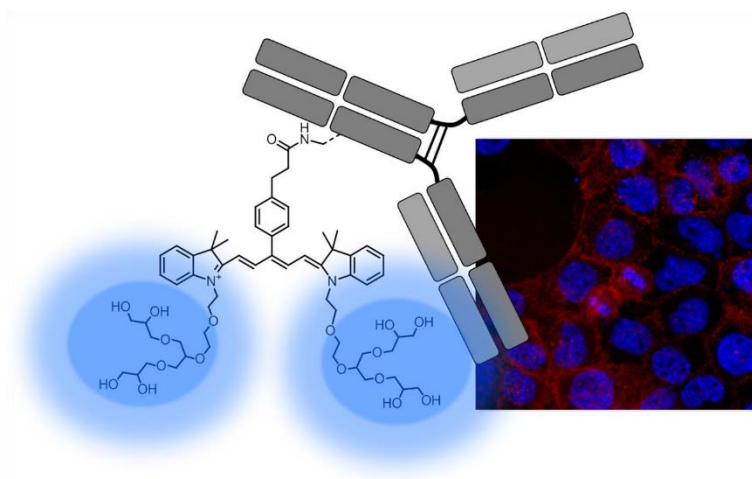


**Figure 37.** Adapted with permission from Wycisk et al.<sup>[114]</sup> Copyright 2015 American Chemical Society.

The contribution of the author was the synthesis of precursors, dyes, and bioconjugates reported in the publication. The author performed with the assistance of Dr. Jutta Pauli the spectroscopic characterization and data evaluation. The manuscript was written by the author.



### 3.2 Responsive Contrast Agents: Synthesis and Characterization of a Tunable Series of pH-Sensitive Near-Infrared pentamethines

Virginia Wycisk\*, Katharina Achazi, Paul Hillmann, Ole Hirsch, Christian Kühne, Jens Dornedde, Rainer Haag, and Kai Licha\* *ACS Omega* **2016**, *1* (5), 808-817.<sup>[115]</sup>

<http://dx.doi.org/10.1021/acsomega.6b00182>

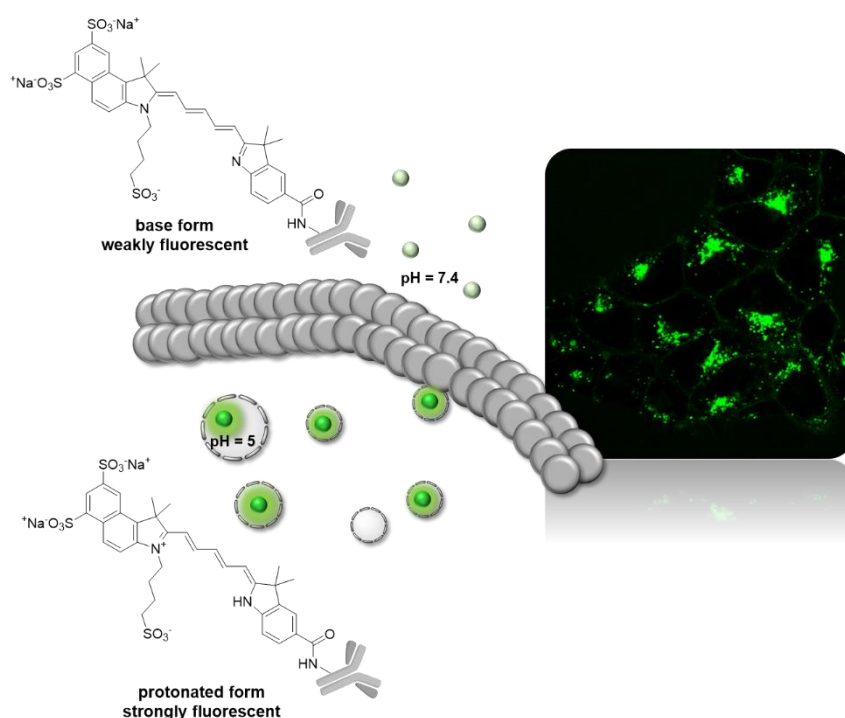


**Figure 38.** Adapted with permission from Wycisk et al.<sup>[115]</sup> Copyright 2016 American Chemical Society.

In this publication, the author contributed with parts of the idea, as well as the synthesis and characterization of the reported dyes and bioconjugates. The author also prepared the manuscript.

### 3.3 Heterobifunctional dyes: Highly Fluorescent Linkers Based on Cyanine Dyes

Virginia Wycisk, Katharina Achazi, Ole Hirsch, Christian Kühne, Jens Dornedde, Rainer Haag, and Kai Licha\*, *ChemistryOpen* **2017**.<sup>[116]</sup>

<http://dx.doi.org/10.1002/open.201700013>

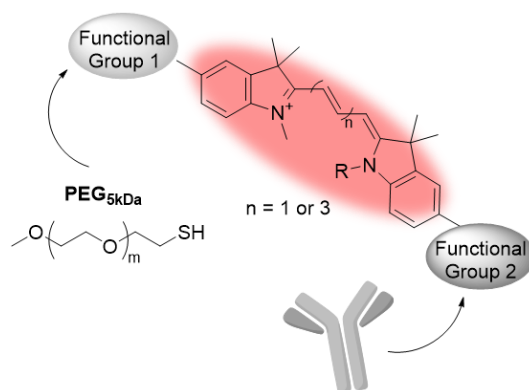


**Figure 39.** Adapted with permission from Wycisk et. al.<sup>[116]</sup>

In this publication, the author contributed with parts of the idea, the synthesis and characterization of heterobifunctional dyes and their bioconjugates, and preparation of the manuscript.

## 4 SUMMARY AND CONCLUSION

This work presented the synthesis and characterization of a novel set of cyanine dyes potentially applicable for biomedical applications in the field of diagnostics and imaging. All dyes were modified at different positions in their chemical structure to suppress aggregation, optimize spectroscopic properties, establish responsiveness to external stimuli, and to incorporate specific moieties for highly specific labeling applications.

In the first part of this thesis, cyanine dyes were synthesized with N-substituted generation 1 glycerol-based dendron building blocks [G1.0] to benefit from their water solubilizing properties and moreover to suppress aggregation due to steric repulsion.<sup>[112-113, 117]</sup> Glycerol-based dendron moieties were modified with three linker motifs and attached to an indolenine moiety via nucleophilic substitution. Condensation with a polymethine forming reagent yielded pentamethine dyes equipped with a total of eight hydroxyl groups. Spectroscopic characterization of dendronized dyes and an analog with classical sulfobutyl pattern revealed enhanced  $\phi_f$  values of up to 0.15 for all synthesized derivatives. Moreover, a cyanine dye containing defined polyethylene glycol (PEG) substitution revealed similar results. Surprisingly, molar absorption coefficients were strongly influenced by the nature of linker connecting the dendron moieties with the indolenine unit. The classical sulfoalkyl dye, (G1.0)-pentyl- and PEG-10 substituted dyes revealed similar coefficients, which were strongly enhanced compared to the other dendronized dyes. Furthermore, the dyes were converted into their respective NHS esters and subsequently conjugated to the monoclonal antibody cetuximab, an antibody targeting the epidermal growth factor receptor (EGFR) on tumor cells, which is clinically established for the treatment of cancer and a well characterized tool for bioconjugation.<sup>[118]</sup> Upon conjugation, increased fluorescence quantum yields were obtained for dyes with ether linkage and exceeded the values of the free dyes even at high D/P ratios above 1. In contrast, conjugated dyes with alkyl-substitution pattern revealed decreased fluorescence quantum yields. Moreover, as opposed to cyanines with classical sulfobutyl pattern, the dendronized dyes showed less tendency to form aggregates when conjugated to cetuximab confirming their suitability as powerful labels for optical imaging techniques.

The second part of this work was focused on the synthesis of responsive cyanine dyes for the investigation of cellular uptake pathways. By applying non-substituted indolenine precursors in asymmetric cyanine synthesis, dyes with pH-sensing properties were obtained. Based on this type of asymmetric pentamethines, derivatives with a total of three sulfonic acid groups were prepared showing excellent water solubility and less aggregation. The attachment of a benzene moiety to the heterocyclic system shifted absorption and fluorescence maximum

close to the optical window which is favorable due to the maximum penetration depth of light.<sup>[119]</sup> Furthermore, pH-sensitive dyes with different *meso*-substitutions were prepared leading to tunable pH responsiveness with respect to the pK<sub>a</sub> values. The incorporation of an electron-withdrawing chlorine atom decreased the pK<sub>a</sub> value to a physiological relevant range. Spectroscopic characterization revealed good optical properties; a strong influence of the *meso*-substitution was observed as  $\phi_f$  increased for non-substituted dyes. By conjugation to cetuximab, we yielded pH-sensitive antibody conjugates for the investigation of cellular uptake kinetics. Confocal laser scanning microscopy (cLSM) confirmed the conjugate functionality as a pronounced signal was observed inside the cells. The dyes with tunable pH dependency clearly demonstrated “turn-On” behavior upon intracellular drop of pH and even revealed differentiated results in cell studies. Whereas the chloro-substituted dye was only giving fluorescence signals inside the cell due to a decreased pK<sub>a</sub> value (7.1), the non-substituted dye with higher pK<sub>a</sub> already visualized the characteristic receptor binding of cetuximab on the cell membrane. Both pH-sensitive dyes revealed low background signal in cellular medium confirming their suitability as powerful labels with tunable pH dependence.

In the third project, cyanine dyes were equipped with different functional groups for the application as fluorescent bifunctional linkers connecting two macromolecules. Information on polymer loading is a difficult but crucial analytical challenge when modifying antibodies with PEG to enhance their blood circulation time *in vivo*. An application of a fluorescent linker could for example permit to gain information on the polymer loading of antibodies when increasing their size by PEG attachment. The major challenge in this project was the synthesis of cyanine dyes with different functional groups directly attached to the aromatic system that is connected to the conjugated  $\pi$ -system. Amino and carboxyl indolenine precursors were condensed with electrophilic reagents ( $n = 1$  or  $2$ ) to form tri- and pentamethine dyes. Moreover, the dyes were equipped with different N-substitution patterns: the classical sulfobutyl groups and, based on the success of the first project, a PEG-10 chain was incorporated to suppress aggregation. In order to obtain a heterobifunctional version of a cyanine dye, a maleimido functionality was introduced into the dye, whereas the other side was converted into an active ester. Subsequent conjugation with the well-studied cetuximab yielded bioconjugates for cellular uptake studies. As further conjugation with PEG<sub>5kDa</sub> thiols via Michael addition failed to succeed, the polymers were attached to the dyes before bioconjugation and revealed nearly full conversion. Subsequent conversion to active ester of the resulting dye-PEG conjugates and bioconjugation with cetuximab yielded polymer-labeled antibodies with incorporated fluorophore at optimal D/P ratios. Complete characterization of optical properties revealed good molar absorption

coefficients and moderate fluorescence quantum yields that were suitable for optical imaging and microscopic detection. Gel electrophoresis confirmed the conjugation of antibodies with dye-labeled polymers by displaying a mass shift of about 5 kDa. Furthermore, cell studies demonstrated the typical receptor binding of the antibody on tumor cells as well as the cellular uptake by signal accumulation inside the cell. These results strengthen the use of heterobifunctional cyanine dyes as suitable fluorescent linkers with fluorescence emission properties.

## 5 OUTLOOK

The enormous possibilities of synthetic modifications of cyanine dyes towards their physicochemical and spectroscopic properties were presented in three different projects.

In the first project, [G1.0] dendronized-cyanine dyes were achieved by alkylation of heterocyclic nitrogen atoms, which yielded pentamethine dyes with improved properties. A stepwise increase of the dendron generation up to [G3.0] extended the number of total hydroxyl groups, which might further decrease aggregation tendencies. This might be particularly helpful for NIR dyes with extended  $\pi$  electronic system, since such heptamethine dyes are even more prone to form aggregates and their application in optical imaging is hampered by low fluorescence quantum yield. Thus, combining hydrophilic dendron moieties with NIR dyes might enhance their optical properties and would generate powerful labels for *in vivo* optical imaging. Another approach follows the conventional concept of incorporating negative charge (either by sulfonate or sulfate moieties) on the periphery to decrease aggregation tendencies by electrostatic repulsion. Sulfation methods have been shown to increase water solubility and to reduce aggregation in aqueous solvents of polymers based on polyglycerol.<sup>[120]</sup> By applying sulfation methods to dendronized dyes, a total of eight sulfate groups could be incorporated into a dye molecule, whereas nowadays a maximum of four sulfonic acids can be placed at the indolenine groups of cyanine dyes.

The second project showed the potential of cyanine dyes to be used as pH sensors and their pH-tunability by structural modifications. Further studies include the conjugation to polymeric scaffolds for the investigation of cellular uptake pathways. Conjugated pH sensors can provide insights on the cellular distribution, as the label and carrier system are located in the same area. This helps to improve drug delivery systems where the drug is supposed to be released in a certain intracellular area which often lacks of unmistakable identification. Furthermore, conjugated pH sensors can provide information on skin penetration or tumor accumulation where pH values vary from the physiological ones.

In the third project, a heterobifunctional cyanine dye was applied as a fluorescent linker by selectively conjugating it with polymers and biomolecules. Further studies include the extension of the structural space by establishing and combining further chemical moieties. For example, ligands for the complexation of radioactive nuclides, such as copper ( $^{64}\text{Cu}$ ) or gallium ( $^{68}\text{Ga}$ ) can be covalently attached to the heterobifunctional dye. Subsequent conjugation to a carrier system leads to a structure for multimodal imaging, a technique which combines optical imaging with positron emission tomography in the case of the nuclides mentioned above. Therefore the probe would enable the simultaneous measurement of two types of emission

signals in different imaging modalities. Furthermore, the incorporation of fluorescent linkers into drug delivery systems can provide information on drug loading as well as on cellular fate of incorporated drugs, potentially utilizing the fluorescence to track drug delivery and release.

## 6 KURZZUSAMMENFASSUNG

Die vorliegende Arbeit präsentiert die Synthese und Charakterisierung von neuen Cyaninfarbstoffen für die potentielle Anwendung in der diagnostischen Bildgebung. Durch gezielte Modifikation konnten die Farbstoffe hinsichtlich ihrer chemischen Eigenschaften wie Aggregationverminderung und spektroskopische Parameter optimiert werden. Weiterhin wurde ein System mit responsiven Eigenschaften auf externe Stimuli etabliert und spezielle Funktionalitäten für hochspezifische Markierungen eingeführt.

Im ersten Teil dieser Arbeit wurden Cyaninfarbstoffe hergestellt, die eine Stickstoffsubstitution mittels Glycerol-basierten Dendroneinheiten der ersten Generation [G1.0] aufwiesen, um von deren löslichkeitsvermittelnden und aggregationsvermindernden Eigenschaften durch sterische Hinderung zu profitieren.<sup>[112-113,117]</sup> Hierbei wurden drei verschiedene Linkerstrukturen zwischen den Dendroneinheiten und dem Indolenin eingeführt, um durch Kondensation mit elektrophilen Reagenzien symmetrische Pentamethine mit insgesamt acht Hydroxylgruppen herzustellen. Weiterhin wurde zum Vergleich ein Farbstoff mit einer Poly(ethylenglycol)kette (PEG) synthetisiert. Bei der spektroskopischen Charakterisierung wurden für alle synthetisierten Farbstoffe Fluoreszenzquantenausbeuten ( $\phi_f$ ) von 0.15 ermittelt. Vergleichend zeigte ein analoger Farbstoff mit klassischer Sulfobutyl-Substitution deutlich kleinere  $\phi_f$ -Werte. Überraschenderweise wurden die molaren Absorptionskoeffizienten stark von der Natur des Linkers zwischen Indolenin- und Dendroneinheit beeinflusst und zeigten die höchsten Werte bei Farbstoffen ohne Heteroatome in der verbindenden Kette. Für weiterführende biologische Studien wurden die Farbstoffe an den monoklonalen Antikörper Cetuximab gekoppelt, der den „epidermal growth factor“ (EGF)-Rezeptor von Tumorzellen bindet und in der Klinik zur Behandlung von Krebs etabliert wurde. Nach der Biokonjugation konnte eine deutliche Erhöhung der Quantenausbeute für Farbstoffe mit Heteroatomen in der Alkylkette ermittelt werden, während der Vergleichsfarbstoff mit Sulfobutylkette niedrigere Quantenausbeuten aufwies. Die Einführung von Dendroneinheiten in Cyaninfarbstoffe führte zu einer deutlichen Verbesserung der optischen Eigenschaften und weniger Aggregation in Biokonjugaten. Die neuen Farbstoffe mit Dendroneinheiten bilden somit eine neue Klasse von Fluorophoren mit optimierten Eigenschaften für die optische Bildgebung.

Der Fokus des zweiten Projektes lag auf der Synthese von responsiven Cyaninfarbstoffen für die Aufklärung von zellulären Aufnahmewegen. Als Ausgangsstoffe wurden Indolenine mit fehlender Alkylierung am Stickstoff gewählt um einen asymmetrischen Farbstoff mit pH-sensitiven Eigenschaften herzustellen. Basierend auf Pentamethinen, wurden



asymmetrische Farbstoffe mit drei Sulfonsäuregruppen hergestellt, die eine hohe Wasserlöslichkeit und geringe Aggregation aufwiesen. Eine zusätzliche Benzoleinheit am Heterozyklus verschob die Absorptions- und Fluoreszenzmaxima näher an das optische Fenster, welches aufgrund der maximalen Eindringtiefe von Licht im Gewebe favorisiert ist. Weiterhin führte die Einführung eines elektronenziehenden Chloratoms an der *meso*-Position, dem zentralen Kohlenstoffatom der Polymethinkette, zu einer Verringerung des  $pK_a$ -Wertes auf 7.1 unterhalb des physiologischen pH-Wertes von 7.5. Die neu hergestellten Farbstoffe mit guten optischen Eigenschaften wurden an Cetuximab gekoppelt und mittels konfokaler „Laser scanning“ Mikroskopie wurde die endozytotische Aufnahme bestätigt. Die Farbstoffkonjugate mit Sensoreigenschaften zeigten ein verstärktes Emissionssignal innerhalb der Zelle im Vergleich zu einem geringen Hintergrundsignal im Zellmedium aufgrund der nicht-fluoreszierenden, deprotonierten Form des Farbstoffs. Während der Chlor-substituierte Farbstoff nur innerhalb der Zelle aufgrund seines niedrigeren  $pK_a$ -Wertes (7.1) fluoreszierte, konnte der nicht-substituierte Farbstoff mit höherem  $pK_a$ -Wert sogar die charakteristische Rezeptorbindung von Cetuximab an die Zellmembran zeigen. Die beiden pH-sensitiven Farbstoffe mit schaltbarer pH-Abhängigkeit überzeugten als Marker für Biomoleküle und konnten den zellulären Aufnahmeweg durch Endozytose veranschaulichen.

Im dritten Projekt, wurden Cyaninfarbstoffe mit verschiedenen funktionellen Gruppen ausgestattet um als fluoreszierende Zwischeneinheit bei der Vernetzung von Makromolekülen zu fungieren. Die Information über den Beladungsgrad an Makromolekülen ist eine schwierige aber wichtige analytische Herausforderung, wenn Antikörper mit PEG beladen werden, um ihre Größe zu erhöhen und damit die Ausscheidung über die Niere zu verhindern. Die heterobifunktionalen Cyaninfarbstoffe wurden ausgehend von Indoleninen mit unterschiedlicher Substitution direkt am aromatischen System hergestellt um einen möglichst rigiden Linker zu erhalten. Bei der Kondensation mit verschiedenen elektrophilen Reagenzien ( $n = 1$  oder  $2$ ) wurden Tri- oder Pentamethine erhalten, die wiederum jeweils mit unterschiedlicher N-Substitution ausgestattet wurden, um die Wasserlöslichkeit zu erhöhen. Basierend auf den Erfolg des ersten Projektes wurde hier eine PEG-10-Kette eingebaut, um eine flexible Löslichkeit zu erzielen. In einer zweistufigen Synthese erfolgte die Modifizierung der terminalen Gruppen zu Maleimid- und NHS-Funktionen, um einen heterobifunktionalen Linker mit starker Reaktivität in biologischem Medium zu erhalten. Die weiterführende Kopplung von PEG<sub>5kDa</sub>-Thiolen mittels Michael-Addition und deren Kopplung an den gut studierten Antikörper Cetuximab ergab die gewünschten, mit einem Polymer markierten Antikörper mit optimalen Beladungsgraden. Die vollständige Charakterisierung der optischen

Eigenschaften ergab gute molare Absorptionskoeffizienten und moderate Fluoreszenzquantenausbeuten, die für die optische Bildgebung und mikroskopische Detektion ausreichend waren. Mittels Gelelektrophorese konnte die kovalente Modifizierung der Antikörper durch eine Massenveränderung von 5 kDa bestätigt werden. Weiterhin bestätigten Zellstudien sowohl die typische Zellmembranbindung von Antikörpermolekülen an Tumorzellen als auch die endozytotische Aufnahme. Die Ergebnisse bekräftigen die Anwendung von Cyaninfarbstoffen als heterobifunktionale Linker mit guten Fluoreszenzeigenschaften.

## 7 REFERENCES

- [1] M. Ormö, A. B. Cubitt, K. Kallio, L. A. Gross, R. Y. Tsien, S. J. Remington, *Science* **1996**, *273*, 1392-1395.
- [2] J. R. Lakowicz, in *Introduction to Fluorescence, Principles of Fluorescence Spectroscopy*, 3rd ed., Springer, **2006**, pp. 1-26.
- [3] J. W. Lichtman, J.-A. Conchello, *Nat Meth* **2005**, *2*, 910-919.
- [4] E. A. Jares-Erijman, T. M. Jovin, *Nat Biotech* **2003**, *21*, 1387-1395.
- [5] J. R. Lakowicz, in *Fluorophores, Principles of Fluorescence Spectroscopy*, Springer US, **2006**, pp. 63-95.
- [6] K. Licha, U. Resch-Genger, *Comprehensive Biomedical Physics*, Elsevier, Oxford, **2014**, pp. 85-109.
- [7] G. T. Hermanson, *Bioconjugate Techniques (Third edition)*, Academic Press, Boston, **2013**, pp. 867-920.
- [8] S. W. Hell, J. Wichmann, *Opt. Lett.* **1994**, *19*, 780-782.
- [9] B. E. Schaafsma, J. S. D. Mieog, M. Hutteman, J. R. van der Vorst, P. J. K. Kuppen, C. W. G. M. Löwik, J. V. Frangioni, C. J. H. van de Velde, A. L. Vahrmeijer, *Journal of Surgical Oncology* **2011**, *104*, 323-332.
- [10] S. G. Werner, H.-E. Langer, S. Ohrndorf, M. Bahner, P. Schott, C. Schwenke, M. Schirner, H. Bastian, G. Lind-Albrecht, B. Kurtz, G. R. Burmester, M. Backhaus, *Annals of the Rheumatic Diseases* **2012**, *71*, 504-510.
- [11] K. Licha, U. Resch-Genger, *Drug Discovery Today: Technologies* **2011**, *8*, e87-e94.
- [12] D. D. Nolting, J. C. Gore, W. Pham, *Current organic synthesis* **2011**, *8*, 521-534.
- [13] V. Pansare, S. Hejazi, W. Faenza, R. K. Prud'homme, *Chemistry of materials : a publication of the American Chemical Society* **2012**, *24*, 812-827.
- [14] A. P. Gorka, R. R. Nani, M. J. Schnermann, *Organic & Biomolecular Chemistry* **2015**, *13*, 7584-7598.
- [15] P. E. Stanga, J. I. Lim, P. Hamilton, *Ophthalmology* **2003**, *110*, 15-21.
- [16] M. V. Marshall, J. C. Rasmussen, I. C. Tan, M. B. Aldrich, K. E. Adams, X. Wang, C. E. Fife, E. A. Maus, L. A. Smith, E. M. Sevick-Muraca, *Open surgical oncology journal (Online)* **2010**, *2*, 12-25.
- [17] H. Kobayashi, P. L. Choyke, *Accounts of Chemical Research* **2011**, *44*, 83-90.
- [18] H. G. Lidell, R. Scott, *A Greek-English Lexicon*,  
[www.perseus.tufts.edu/hopper/text?doc=Perseus%3Atext%3A1999.04.0057%3Aentry%3Dku%2Fanos](http://www.perseus.tufts.edu/hopper/text?doc=Perseus%3Atext%3A1999.04.0057%3Aentry%3Dku%2Fanos)

- [19] C. H. G. Williams, *Trans. R. Soc. Edinburgh* **1856**, *21*, 377-401.
- [20] R. M. Christie, *Colour Chemistry* (Ed.: R. M. Christie), The Royal Society of Chemistry, **2001**, pp. 102-117.
- [21] M. Mojzych, M. Henary, *Heterocyclic Polymethine Dyes: Synthesis, Properties and Applications* (Ed.: L. Strekowski), Springer Berlin Heidelberg, Berlin, Heidelberg, **2008**, pp. 1-9.
- [22] E. Kim, S. B. Park, *Advanced Fluorescence Reporters in Chemistry and Biology I: Fundamentals and Molecular Design* (Ed.: A. P. Demchenko), Springer Berlin Heidelberg, Berlin, Heidelberg, **2010**, pp. 149-186.
- [23] L. A. Ernst, R. K. Gupta, R. B. Mujumdar, A. S. Waggoner, *Cytometry* **1989**, *10*, 3-10.
- [24] E. Soriano, C. Holder, A. Levitz, M. Henary, *Molecules* **2016**, *21*, 23.
- [25] C. Holzhauser, S. Berndl, F. Menacher, M. Breunig, A. Göpferich, H.-A. Wagenknecht, *European Journal of Organic Chemistry* **2010**, *2010*, 1239-1248.
- [26] P. F. Gordon, P. Gregory, *Organic Chemistry in Colour*, Springer Berlin Heidelberg, Berlin, Heidelberg, **1987**, pp. 200-261.
- [27] P. Chen, S. Sun, Y. Hu, Z. Qian, D. Zheng, *Dyes and Pigments* **1999**, *41*, 227-231.
- [28] G. A. Reynolds, K. H. Drexhage, *The Journal of Organic Chemistry* **1977**, *42*, 885-888.
- [29] M. Henary, M. Mojzych, *Heterocyclic Polymethine Dyes: Synthesis, Properties and Applications* (Ed.: L. Strekowski), Springer Berlin Heidelberg, Berlin, Heidelberg, **2008**, pp. 221-238.
- [30] L. Strekowski, M. Lipowska, G. Patonay, *Synthetic Communications* **1992**, *22*, 2593-2598.
- [31] D. M. Sturmer, *Chemistry of Heterocyclic Compounds*, John Wiley & Sons, Inc., **2008**, pp. 441-587.
- [32] U. De Rossi, J. Moll, M. Spieles, G. Bach, S. Dähne, J. Kriwanek, M. Lisk, *Journal für Praktische Chemie/Chemiker-Zeitung* **1995**, *337*, 203-208.
- [33] K. Licha, C. Hessenius, A. Becker, P. Henklein, M. Bauer, S. Wisniewski, B. Wiedenmann, W. Semmler, *Bioconjugate Chemistry* **2001**, *12*, 44-50.
- [34] A. I. M. Koraiem, Z. H. Khalil, R. M. Abu El-Hamd, *Dyes and Pigments* **1990**, *13*, 289-299.
- [35] M. E. Jung, W.-J. Kim, *Bioorganic & Medicinal Chemistry* **2006**, *14*, 92-97.
- [36] R. B. Mujumdar, L. A. Ernst, S. R. Mujumdar, A. S. Waggoner, *Cytometry* **1989**, *10*, 11-19.

- [37] P. L. Southwick, L. A. Ernst, E. W. Tauriello, S. R. Parker, R. B. Mujumdar, S. R. Mujumdar, H. A. Clever, A. S. Waggoner, *Cytometry* **1990**, *11*, 418-430.
- [38] R. B. Mujumdar, L. A. Ernst, S. R. Mujumdar, C. J. Lewis, A. S. Waggoner, *Bioconjugate Chemistry* **1993**, *4*, 105-111.
- [39] S. R. Mujumdar, R. B. Mujumdar, C. M. Grant, A. S. Waggoner, *Bioconjugate Chemistry* **1996**, *7*, 356-362.
- [40] S. M. B. Makin, I. I.; Shavrygina, O. A, *Zhurnal Organicheskoi Khimii* **1977** *13*, 2440-2443.
- [41] N. Narayanan, G. Patonay, *The Journal of Organic Chemistry* **1995**, *60*, 2391-2395.
- [42] L. Strekowski, J. C. Mason, J. E. Britton, H. Lee, K. Van Aken, G. Patonay, *Dyes and Pigments* **2000**, *46*, 163-168.
- [43] H. Mitekura, T. No, K. Suzuki, K. Satake, M. Kimura, *Dyes and Pigments* **2002**, *54*, 113-120.
- [44] H.-H. Johannes, W. Grahn, A. Reisner, P. G. Jones, *Tetrahedron Letters* **1995**, *36*, 7225-7228.
- [45] J. H. Flanagan, S. H. Khan, S. Menchen, S. A. Soper, R. P. Hammer, *Bioconjugate Chemistry* **1997**, *8*, 751-756.
- [46] J. D. L. Gallaher, M. E. Johnson, *Analyst* **1999**, *124*, 1541-1546.
- [47] F. Song, X. Peng, E. Lu, Y. Wang, W. Zhou, J. Fan, *Tetrahedron Letters* **2005**, *46*, 4817-4820.
- [48] F. Song, X. Peng, E. Lu, R. Zhang, X. Chen, B. Song, *Journal of Photochemistry and Photobiology A: Chemistry* **2004**, *168*, 53-57.
- [49] L. Strekowski, C. J. Mason, H. Lee, R. Gupta, J. Sowell, G. Patonay, *Journal of Heterocyclic Chemistry* **2003**, *40*, 913-916.
- [50] N. Miyaura, A. Suzuki, *Chemical Reviews* **1995**, *95*, 2457-2483.
- [51] H. Lee, J. C. Mason, S. Achilefu, *The Journal of Organic Chemistry* **2008**, *73*, 723-725.
- [52] H. Lee, J. C. Mason, S. Achilefu, *The Journal of Organic Chemistry* **2006**, *71*, 7862-7865.
- [53] J. Pauli, K. Licha, J. Berkemeyer, M. Grabolle, M. Spieles, N. Wegner, P. Welker, U. Resch-Genger, *Bioconjugate Chemistry* **2013**, *24*, 1174-1185.
- [54] H. Illy, L. Funderburk, *The Journal of Organic Chemistry* **1968**, *33*, 4283-4285.
- [55] D. W. Heseltine, J. E. Jones, L. L. Lincoln, *Vol. 3*, US Patent, **1968**, p. 927.

- [56] E. Terpetschnig, H. Szmacinski, A. Ozinskas, J. R. Lakowicz, *Analytical Biochemistry* **1994**, *217*, 197-204.
- [57] K. Licha, B. Riefke, V. Ntziachristos, A. Becker, B. Chance, W. Semmler, *Photochemistry and Photobiology* **2000**, *72*, 392-398.
- [58] D. J. Gale, J. F. K. Wilshire, *Journal of the Society of Dyers and Colourists* **1974**, *90*, 97-100.
- [59] P. L. Southwick, A. S. Waggoner, Google Patents, **1991**.
- [60] B. Chipon, G. Clavé, C. Bouteiller, M. Massonneau, P.-Y. Renard, A. Romieu, *Tetrahedron Letters* **2006**, *47*, 8279-8284.
- [61] J. Klohs, A. Wunder, K. Licha, *Basic Res Cardiol* **2008**, *103*, 144-151.
- [62] J. Pączkowski, J. Kabatc, B. Jędrzejewska, *Heterocyclic Polymethine Dyes: Synthesis, Properties and Applications* (Ed.: L. Strekowski), Springer Berlin Heidelberg, Berlin, Heidelberg, **2008**, pp. 183-220.
- [63] L. D. Patsenker, A. L. Tatarets, E. A. Terpetschnig, *Advanced Fluorescence Reporters in Chemistry and Biology I: Fundamentals and Molecular Design* (Ed.: A. P. Demchenko), Springer Berlin Heidelberg, Berlin, Heidelberg, **2010**, pp. 65-104.
- [64] U. Resch-Genger, M. Grabolle, S. Cavaliere-Jaricot, R. Nitschke, T. Nann, *Nat Meth* **2008**, *5*, 763-775.
- [65] S. M. Yarmoluk, V. B. Kovalska, S. S. Lukashov, Y. L. Slominskii, *Bioorganic & Medicinal Chemistry Letters* **1999**, *9*, 1677-1678.
- [66] V. B. Kovalska, K. D. Volkova, M. Y. Losytskyy, O. I. Tolmachev, A. O. Balanda, S. M. Yarmoluk, *Spectrochimica Acta Part A: Molecular and Biomolecular Spectroscopy* **2006**, *65*, 271-277.
- [67] L. Linck, P. Kapusta, U. Resch-Genger, *Photochemistry and Photobiology* **2012**, *88*, 867-875.
- [68] A. Mishra, R. K. Behera, P. K. Behera, B. K. Mishra, G. B. Behera, *Chemical Reviews* **2000**, *100*, 1973-2012.
- [69] A. Eisfeld, J. S. Briggs, *Chemical Physics* **2006**, *324*, 376-384.
- [70] R. Steiger, R. Pugin, J. Heier, *Colloids and Surfaces B: Biointerfaces* **2009**, *74*, 484-491.
- [71] B. R. Renikuntla, H. C. Rose, J. Eldo, A. S. Waggoner, B. A. Armitage, *Organic Letters* **2004**, *6*, 909-912.
- [72] S. Lepaja, H. Strub, D.-J. Lougnot, in *Zeitschrift für Naturforschung A*, Vol. 38, **1983**, p. 56.

- [73] R. Guether, M. V. Reddington, *Tetrahedron Letters* **1997**, *38*, 6167-6170.
- [74] X. Chen, X. Peng, A. Cui, B. Wang, L. Wang, R. Zhang, *Journal of Photochemistry and Photobiology A: Chemistry* **2006**, *181*, 79-85.
- [75] L. Strekowski, H. Lee, J. C. Mason, M. Say, G. Patonay, *Journal of Heterocyclic Chemistry* **2007**, *44*, 475-477.
- [76] L. Strekowski, M. Lipowska, T. Górecki, J. C. Mason, G. Patonay, *Journal of Heterocyclic Chemistry* **1996**, *33*, 1685-1688.
- [77] L. Strekowski, J. C. Mason, H. Lee, M. Say, G. Patonay, *Journal of Heterocyclic Chemistry* **2004**, *41*, 227-232.
- [78] J. Kabatc, J. Pączkowski, *Dyes and Pigments* **2004**, *61*, 1-16.
- [79] O. Mader, K. Reiner, H.-J. Egelhaaf, R. Fischer, R. Brock, *Bioconjugate Chemistry* **2004**, *15*, 70-78.
- [80] X. Peng, F. Song, E. Lu, Y. Wang, W. Zhou, J. Fan, Y. Gao, *Journal of the American Chemical Society* **2005**, *127*, 4170-4171.
- [81] N. Acar, J. Kurzawa, N. Fritz, A. Stockmann, C. Roman, S. Schneider, T. Clark, *The Journal of Physical Chemistry A* **2003**, *107*, 9530-9541.
- [82] J. Han, K. Burgess, *Chemical Reviews* **2010**, *110*, 2709-2728.
- [83] M. S. Briggs, D. D. Burns, M. E. Cooper, S. J. Gregory, *Chemical Communications* **2000**, 2323-2324.
- [84] S. Miltsov, C. Encinas, J. Alonso, *Tetrahedron Letters* **1998**, *39*, 9253-9254.
- [85] M. Cooper, S. Gregory, E. Adie, S. Kalinka, *Journal of Fluorescence* **2002**, *12*, 425-429.
- [86] Z. Zhang, S. Achilefu, *Chemical Communications* **2005**, 5887-5889.
- [87] R. M. El-Shishtawy, P. Almeida, *Tetrahedron* **2006**, *62*, 7793-7798.
- [88] Y. Xu, Y. Liu, X. Qian, *Journal of Photochemistry and Photobiology A: Chemistry* **2007**, *190*, 1-8.
- [89] S. A. Hilderbrand, K. A. Kelly, M. Niedre, R. Weissleder, *Bioconjugate Chemistry* **2008**, *19*, 1635-1639.
- [90] M. J. Patrick, J. M. Janjic, H. Teng, M. R. O'Hear, C. W. Brown, J. A. Stokum, B. F. Schmidt, E. T. Ahrens, A. S. Waggoner, *Journal of the American Chemical Society* **2013**, *135*, 18445-18457.
- [91] B. Tang, X. Liu, K. Xu, H. Huang, G. Yang, L. An, *Chemical Communications* **2007**, 3726-3728.

- [92] B. Tang, F. Yu, P. Li, L. Tong, X. Duan, T. Xie, X. Wang, *Journal of the American Chemical Society* **2009**, *131*, 3016-3023.
- [93] J. S. Kim, R. Kodagahally, L. Strekowski, G. Patonay, *Talanta* **2005**, *67*, 947-954.
- [94] G. Patonay, J. S. Kim, R. Kodagahally, L. Strekowski, *Applied Spectroscopy* **2005**, *59*, 682-690.
- [95] C.-H. Tung, S. Bredow, U. Mahmood, R. Weissleder, *Bioconjugate Chemistry* **1999**, *10*, 892-896.
- [96] J. B. Grimm, L. M. Heckman, L. D. Lavis, *Progress in Molecular Biology and Translational Science, Vol. Volume 113* (Ed.: C. M. May), Academic Press, **2013**, pp. 1-34.
- [97] D. Puliti, D. Warther, C. Orange, A. Specht, M. Goeldner, *Bioorganic & Medicinal Chemistry* **2011**, *19*, 1023-1029.
- [98] W. Sun, S. Guo, C. Hu, J. Fan, X. Peng, *Chemical Reviews* **2016**, *116*, 7768-7817.
- [99] B. Xing, A. Khanamiryan, J. Rao, *Journal of the American Chemical Society* **2005**, *127*, 4158-4159.
- [100] N. Karton-Lifshin, E. Segal, L. Omer, M. Portnoy, R. Satchi-Fainaro, D. Shabat, *Journal of the American Chemical Society* **2011**, *133*, 10960-10965.
- [101] O. Redy-Keisar, E. Kisin-Finfer, S. Ferber, R. Satchi-Fainaro, D. Shabat, *Nat. Protocols* **2014**, *9*, 27-36.
- [102] O. Redy-Keisar, S. Ferber, R. Satchi-Fainaro, D. Shabat, *ChemMedChem* **2015**, *10*, 999-1007.
- [103] B. D'Autreaux, M. B. Toledano, *Nat Rev Mol Cell Biol* **2007**, *8*, 813-824.
- [104] W.-S. Wu, *Cancer Metastasis Rev* **2006**, *25*, 695-705.
- [105] O. Hwang, *Experimental Neurobiology* **2013**, *22*, 11-17.
- [106] M. Valko, D. Leibfritz, J. Moncol, M. T. D. Cronin, M. Mazur, J. Telser, *The International Journal of Biochemistry & Cell Biology* **2007**, *39*, 44-84.
- [107] C. C. Winterbourn, *Nat Chem Biol* **2008**, *4*, 278-286.
- [108] K. Kundu, S. F. Knight, N. Willett, S. Lee, W. R. Taylor, N. Murthy, *Angewandte Chemie International Edition* **2009**, *48*, 299-303.
- [109] S. Selvam, K. Kundu, K. L. Templeman, N. Murthy, A. J. García, *Biomaterials* **2011**, *32*, 7785-7792.
- [110] J.-Y. Kim, W. I. Choi, Y. H. Kim, G. Tae, *Journal of Controlled Release* **2011**, *156*, 398-405.



- [111] D. Oushiki, H. Kojima, T. Terai, M. Arita, K. Hanaoka, Y. Urano, T. Nagano, *Journal of the American Chemical Society* **2010**, *132*, 2795-2801.
- [112] T. Heek, C. Fasting, C. Rest, X. Zhang, F. Wurthner, R. Haag, *Chemical Communications* **2010**, *46*, 1884-1886.
- [113] S. K. Yang, X. Shi, S. Park, S. Doganay, T. Ha, S. C. Zimmerman, *Journal of the American Chemical Society* **2011**, *133*, 9964-9967.
- [114] V. Wycisk, J. Pauli, P. Welker, A. Justies, U. Resch-Genger, R. Haag, K. Licha, *Bioconjugate Chemistry* **2015**, *26*, 773-781.
- [115] V. Wycisk, K. Achazi, P. Hillmann, O. Hirsch, C. Kuehne, J. Dervedde, R. Haag, K. Licha, *ACS Omega* **2016**, *1*, 808-817.
- [116] V. Wycisk, K. Achazi, O. Hirsch, C. Kuehne, J. Dervedde, R. Haag, K. Licha, **2016**.
- [117] T. Heek, J. Nikolaus, R. Schwarzer, C. Fasting, P. Welker, K. Licha, A. Herrmann, R. Haag, *Bioconjugate Chemistry* **2013**, *24*, 153-158.
- [118] S.-F. Wong, *Clinical Therapeutics* **2005**, *27*, 684-694.
- [119] A. M. Smith, M. C. Mancini, S. Nie, *Nat Nano* **2009**, *4*, 710-711.
- [120] M. Weinhart, D. Gröger, S. Enders, J. Dervedde, R. Haag, *Biomacromolecules* **2011**, *12*, 2502-2511.

## 8 APPENDIX

### 8.1 List of Abbreviations

BODIPY	Boron-Dipyrromethene
cLSM	Confocal laser scanning microscopy
EGFR	Epidermal Growth Factor Receptor
ELISA	Enzyme-linked immosorbent assay
FRET	Förster Resonance Energy Transfer
GFP	Green Fluorescent Protein
H <sub>2</sub> O <sub>2</sub>	Hydrogen peroxide
HO·	Hydroxyl radical
HSA	Human Serum Albumin
ICC	Indocarbocyanine
ICG	Indocyanine Green
ICT	Intramolecular charge transfer
IDCC	Indodicarbocyanine
ITCC	Indotricarbocyanine
LPS	Lipopolysaccharide
NHS	N-Hydroxysuccinimide
NIR	Near-Infrared
O <sub>2</sub> <sup>-</sup>	Superoxide anion
PEG	Poly(ethylene glycol)
PeT	Photon-induced electron transfer
ROS	Reactive Oxygen Species
S <sub>0</sub>	Ground state
S <sub>1</sub>	First excited state
S <sub>2</sub>	Second excited state
S <sub>N</sub>	Nucleophilic Substitution
SNR	Signal-to-noise ratio
S <sub>RN1</sub>	Radical nucleophilic substitution
STED	Stimulated Emission Depletion
VIS	Visible
ε	Molar absorption coefficient
φ <sub>f</sub>	Fluorescence quantum yield

## 8.2 List of Publications

- 1) **Wycisk, V.**; Pauli, J.; Welker, P.; Justies, A.; Resch-Genger, U.; Haag, R.; Licha, K. Glycerol-Based Contrast Agents: A Novel Series of Dendronized Pentamethine Dyes. *Bioconjugate Chemistry* **2015**, *26* (4), 773-781.
- 2) Donskyi, I.; Achazi, K.; **Wycisk, V.**; Boettcher, C.; Adeli, M. Synthesis, self-assembly, and photocrosslinking of fullerene-polyglycerol amphiphiles as nanocarriers with controlled transport properties. *Chemical Communications* **2016**, *52* (23), 4373-4376.
- 3) **Wycisk, V.**; Achazi, K.; Hillmann, P.; Hirsch, O.; Kuehne, C.; Dervedde, J.; Haag, R.; Licha, K. Responsive Contrast Agents: Synthesis and Characterization of a Tunable Series of pH-Sensitive Near-Infrared Pentamethines. *ACS Omega* **2016**, *1* (5), 808-817.
- 4) Dimde, M.; Sahle, F.; **Wycisk, V.**; Steinhilber, D.; Camacho, L. C.; Licha, K.; Lademann, J.; Haag, R., Determination of hair follicle pH values using novel pH-nanosensors, **2016** *submitted*.
- 5) **Wycisk, V.**; Achazi, K.; Hirsch, O.; Kuehne, C.; Dervedde, J.; Haag, R.; Licha, K. Heterobifunctional dyes: Highly Fluorescent Linkers Based on Cyanine Dyes, **2016**, *submitted*.

## 8.3 Manuscripts in Preparation

- 1) Kepsutlu, B.; **Wycisk, V.**; Achazi, K.; Vonnemann, J.; Ballauff, M.; Haag, R.; Schneider, G.; McNally, J. Near-native state imaging and quantitative analysis of cellular trafficking of dendritic polyglycerol sulfate
- 2) Donskyi, I.; Achazi, K.; **Wycisk, V.**; Licha, K.; Adeli, M.\*; Haag, R.\* Fullerene Polyglycerol Amphiphiles as New Vectors for Biomedical Applications

## **8.4 Curriculum Vitae**

Der Lebenslauf ist aus Gründen des Datenschutzes nicht enthalten.